

This is an Open Access document downloaded from ORCA, Cardiff University's institutional repository: <https://orca.cardiff.ac.uk/id/eprint/103281/>

This is the author's version of a work that was submitted to / accepted for publication.

Citation for final published version:

Khaki, M., Schumacher, M., Forootan, Ehsan, Kuhn, M., Awange, J.L. and van Dijk, A. I. J. M. 2017. Accounting for spatial correlation errors in the assimilation of GRACE into hydrological models through localization. *Advances in Water Resources* 108, pp. 99-112. 10.1016/j.advwatres.2017.07.024

Publishers page: <http://dx.doi.org/10.1016/j.advwatres.2017.07.024>

Please note:

Changes made as a result of publishing processes such as copy-editing, formatting and page numbers may not be reflected in this version. For the definitive version of this publication, please refer to the published source. You are advised to consult the publisher's version if you wish to cite this paper.

This version is being made available in accordance with publisher policies. See <http://orca.cf.ac.uk/policies.html> for usage policies. Copyright and moral rights for publications made available in ORCA are retained by the copyright holders.

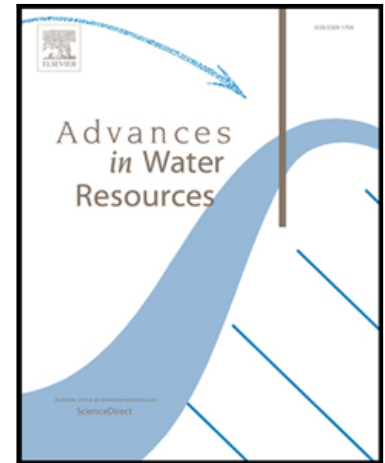


Accepted Manuscript

Accounting for Spatial Correlation Errors in the Assimilation of GRACE into Hydrological Models through localization

M. Khaki, M. Schumacher, E. Forootan, M. Kuhn, J.L. Awange, A.I.J.M. van Dijk

PII: S0309-1708(16)30816-8
DOI: [10.1016/j.advwatres.2017.07.024](https://doi.org/10.1016/j.advwatres.2017.07.024)
Reference: ADWR 2909



To appear in: *Advances in Water Resources*

Received date: 23 December 2016
Revised date: 31 July 2017
Accepted date: 31 July 2017

Please cite this article as: M. Khaki, M. Schumacher, E. Forootan, M. Kuhn, J.L. Awange, A.I.J.M. van Dijk, Accounting for Spatial Correlation Errors in the Assimilation of GRACE into Hydrological Models through localization, *Advances in Water Resources* (2017), doi: [10.1016/j.advwatres.2017.07.024](https://doi.org/10.1016/j.advwatres.2017.07.024)

This is a PDF file of an unedited manuscript that has been accepted for publication. As a service to our customers we are providing this early version of the manuscript. The manuscript will undergo copyediting, typesetting, and review of the resulting proof before it is published in its final form. Please note that during the production process errors may be discovered which could affect the content, and all legal disclaimers that apply to the journal pertain.

Accounting for Spatial Correlation Errors in the Assimilation of GRACE into Hydrological Models through localization

M. Khaki^{a,1}, M. Schumacher^b, E. Forootan^{a,c}, M. Kuhn^a, J. L. Awange^a, A. I. J. M. van Dijk^d

^a*Western Australian Centre for Geodesy and The Institute for Geoscience Research, Curtin University, Perth, Australia.*

^b*School of Geographical Sciences, University of Bristol, Bristol, UK.*

^c*School of Earth and Ocean Sciences, Cardiff University, Cardiff, UK.*

^d*Fenner School of Environment and Society, the Australian National University, Canberra, Australia.*

Abstract

1 Assimilation of terrestrial water storage (TWS) information from the Gravity Recovery And
 2 Climate Experiment (GRACE) satellite mission can provide significant improvements in hydro-
 3 logical modeling. However, the rather coarse spatial resolution of GRACE TWS and its spatially
 4 correlated errors pose considerable challenges for achieving realistic assimilation results. Conse-
 5 quently, successful data assimilation depends on rigorous modelling of the full error covariance
 6 matrix of the GRACE TWS estimates, as well as realistic error behavior for hydrological model
 7 simulations. In this study, we assess the application of local analysis (LA) to maximize the con-
 8 tribution of GRACE TWS in hydrological data assimilation. For this, we assimilate GRACE
 9 TWS into the World-Wide Water Resources Assessment system (W3RA) over the Australian
 10 continent while applying LA and accounting for existing spatial correlations using the full error
 11 covariance matrix. GRACE TWS data is applied with different spatial resolutions including 1°
 12 to 5° grids, as well as basin averages. The ensemble-based sequential filtering technique of the
 13 Square Root Analysis (SQRA) is applied to assimilate TWS data into W3RA. For each spatial
 14 scale, the performance of the data assimilation is assessed through comparison with indepen-
 15 dent in-situ ground water and soil moisture observations. Overall, the results demonstrate that
 16 LA is able to stabilize the inversion process (within the implementation of the SQRA filter)
 17 leading to less errors for all spatial scales considered with an average RMSE improvement of
 18 54% (e.g., 52.23 mm down to 26.80 mm) for all the cases with respect to groundwater in-situ
 19 measurements. Validating the assimilated results with groundwater observations indicates that
 20 LA leads to 13% better (in terms of RMSE) assimilation results compared to the cases with
 21 Gaussian errors assumptions. This highlights the great potential of LA and the use of the full

Email address: Mehdi.Khaki@postgrad.curtin.edu.au (M. Khaki)

¹Contact details: Western Australian Centre for Geodesy and The Institute for Geoscience Research, Curtin University, Perth, Australia, Email: Mehdi.Khaki@postgrad.curtin.edu.au, Tel: 0061410620379

22 error covariance matrix of GRACE TWS estimates for improved data assimilation results.

23

Keywords: Data assimilation, GRACE, Localization, Hydrological model.

24 1. Introduction

25 The Gravity Recovery And Climate Experiment (GRACE) satellite mission provides
26 global time-variable gravity field solutions that have been used to obtain global terrestrial
27 water storage (TWS) changes (Tapley et al., 2004). Several studies indicate that GRACE
28 TWS can play an important role in better understanding surface and sub-surface physical
29 processes related to water redistribution within the Earth system (e.g., Huntington, 2006;
30 Chen et al., 2007; Kusche et al., 2012; Forootan et al., 2014; van Dijk et al., 2014; Wouters
31 et al., 2014). A growing number of studies has also been applying GRACE TWS to constrain
32 the mass balance of hydrological models (e.g., Zaitchik et al., 2008; Thomas et al., 2014;
33 van Dijk et al., 2014; Eicker et al., 2014; Tangdamrongsub et al., 2015; Reager et al., 2015;
34 Khaki et al., 2017). This combination is motivated by the fact that hydrological models use
35 conceptual or physical knowledge (or both) to simulate hydrological processes at global (e.g.,
36 Huntington, 2006; Coumou and Rahmstorf, 2012) and regional (e.g., Zaitchik et al., 2008; Chen
37 et al., 2013; Munier et al., 2014) scales. The accuracy of simulations might be limited due to
38 imperfect models (i.e., lack of knowledge about the processes or simplified model equations) and
39 uncertainties in input and forcing data (Vrugt et al., 2013). Data limitation (both on temporal
40 and spatial scales) also plays a substantial role in land hydrological modeling, especially for
41 closing the water balance that requires reliable information about all storage compartments
42 from which that of groundwater is very challenging. In this regard, GRACE TWS estimates
43 are of great importance since they can be used through data assimilation to constrain the
44 vertical summation of water storages (including groundwater) in the models.

45 Data assimilation is a technique to incorporate observations into a dynamic model in order
46 to improve its state estimation (Bertino et al., 2003; Hoteit et al., 2012). It has been widely
47 applied in the fields of ocean and climate science (Garner et al., 1999; Elbern and Schmidt,
48 2001; Bennett, 2002; Kalnay, 2003; Schunk et al., 2004; Lahoz, 2007; Zhang et al., 2012). In
49 hydrological studies, different in-situ measurements (e.g., river discharge and soil moisture)
50 have been assimilated into models (Liu et al., 2012) to improve their estimates of different

51 hydrological quantities (see, e.g., [Crow and Wood, 2003](#); [Seo et al., 2003](#); [Vrugt et al., 2005](#);
52 [Weerts et al., 2006](#); [Reichle et al., 2010](#)).

53 The application of remotely sensed data in data assimilation for hydrological purposes has
54 gathered interests in the past few years. This is especially due to the increased development and
55 availability of satellite remote sensing systems such as Sentinel, Soil Moisture Active Passive
56 (SMAP), GRACE, and satellite radar altimetry (e.g., [Moradkhani et al., 2006](#); [Clark et al.,
57 2008](#); [Houborg et al., 2012](#); [van Dijk et al., 2014](#); [Renzullo et al., 2014](#); [Reager et al., 2015](#);
58 [Kumar et al., 2016](#)). Data assimilation can improve various water compartments of hydrological
59 models such as soil (e.g., [Reichle et al., 2002, 2008](#); [Brocca et al., 2010](#); [Kumar et al., 2014](#);
60 [Renzullo et al., 2014](#)), surface water (e.g., [Alsdorf et al., 2007](#); [Neal et al., 2009](#); [Giustarini et
61 al., 2011](#)), and snow (e.g., [Liu et al., 2013](#); [Kumar et al., 2015](#)) storages. A number of studies
62 has also investigated the possibility of using GRACE data to improve hydrological models (e.g.,
63 [Zaitchik et al., 2008](#); [Houborg et al., 2012](#); [Li et al., 2012](#); [Eicker et al., 2014](#); [van Dijk et al.,
64 2014](#); [Tangdamrongsub et al., 2015](#); [Kumar et al., 2016](#); [Schumacher et al., 2016](#)).

65 GRACE data with a suitable coverage, both temporally and spatially, provide a unique
66 opportunity to study water storages in lands on global and regional scales. The mission now
67 provides 15 years of data with a global coverage, which provides the chance to study seasonal to
68 decadal changes in TWS. Before using GRACE TWS in any assimilation framework, however,
69 there are some important aspects which should be considered such as the temporal and spatial
70 resolution mismatch between GRACE observations and model simulations, as well as existing
71 spatial and temporal correlations in the time series of GRACE TWS and model simulations.
72 Its spatial resolution is limited to a few hundred kilometers depending on the signal strength
73 and the inversion technique applied to recover time-variable gravity fields ([Schmidt et al.,
74 2008](#)). This coarse spatial resolution exists in both GRACE level 2 solutions provided in
75 terms of spherical harmonics potential coefficients or mass concentration (mascon) solutions.
76 Although mascon is provided on a finer spatial scale (e.g., 0.5°), the native resolution of the
77 data is smaller (e.g., 3° ; [Watkins et al., 2015](#); [Wiese, 2015](#)). Different studies have tried to
78 assimilate GRACE data in either basin scales (e.g., [Zaitchik et al., 2008](#); [Houborg et al., 2012](#);
79 [Li et al., 2012](#)) or grid element scales (e.g., [Eicker et al., 2014](#); [Tangdamrongsub et al., 2015](#);
80 [Schumacher et al., 2016](#)). GRACE level 2 products have been truncated (e.g., at degree and
81 order 60-120). They also have been filtered (e.g., [Swenson and Wahr, 2006](#); [Kusche, 2007](#))

82 resulting in low spatial resolutions. Upscaling of the original established TWS with a limited
83 spatial resolution to create a high spatial resolution data (e.g., 1°) with grid points that are
84 not independent of each other increases spatial correlation significantly (see e.g., [Schumacher
85 et al., 2016](#)). Accounting for these correlations is important especially in the context of data
86 assimilation, where complete knowledge of the data error structure including uncertainties and
87 existing correlations is necessary.

88 Data assimilation as an inverse problem uses the covariance information of model simula-
89 tions and observations. Significantly correlated errors yield covariance matrices that are bad
90 conditioned or not invertible leading to inefficiency in filtering process during data assimilation.
91 Due to the lack of information (or to enhance computations), the decision of uncorrelated data
92 (Gaussian error for observations) is often made to deal with this problem, which can be realis-
93 tic when observations are denser than models' grid, e.g., independent grid points of neighbours
94 ([Berger and Forsythe, 2004](#); [Stewart et al., 2008](#)). In contrast, when the spatial resolution of
95 models is finer than the assimilated observations, it can lead to no improvement in the accuracy
96 of final assimilation results (e.g., [Liu and Rabier, 2003](#); [Dando et al., 2007](#); [Stewart et al., 2008](#)).
97 In this regard, it is necessary to precisely consider the full GRACE error covariance for different
98 spatial resolutions in data assimilation applications especially where the model spatial scale is
99 finer than GRACE TWS, and the existing correlations in the observations are problematic (see
100 e.g., [Schumacher et al., 2016](#)).

101 Most of the previous studies assimilated GRACE TWS (e.g., grid-based or basin aver-
102 aged) into models while assuming white noise (i.e., uncorrelated observations). This, for basin
103 averaged applications, might be justified to some extent as the spatial averaging of TWS ob-
104 servations adds up the non-Gaussian noise distributions and generates a mixture that is closer
105 to Gaussian distribution according to the central limit theorem ([Stone, 2004](#), Chapter 5). In
106 this regard, for example, [Zaitchik et al. \(2008\)](#) applied GRACE TWS on a sub-basin scale
107 (sub-basins of the Mississippi River) and assumed a Gaussian error (with zero correlation)
108 for GRACE TWS measurements. [Reichle et al. \(2013\)](#) investigated the effects of coarse-scale
109 satellite observations (e.g., GRACE) and vertically integrated measurements (such as TWS) on
110 model variables within the assimilation system. For a grid-based assimilation of GRACE-TWS
111 in models, [Eicker et al. \(2014\)](#) studied the relationship of different GRACE spatial resolutions
112 on the data assimilation process and reported that there is always a trade-off between em-

113 ploying GRACE data in a higher spatial resolution while keeping the GRACE error covariance
114 matrices reasonably well conditioned. [Giroto et al. \(2016, 2017\)](#) have considered the fact that
115 1° GRACE error covariances are spatially highly correlated and to address this issue, they have
116 used a spatial correlation length of 3° for the observation errors (see also [Kumar et al., 2016](#);
117 [Khaki et al., 2017](#)). [Schumacher et al. \(2016\)](#) indicated that both the characteristics of GRACE
118 error correlation and spatial discretization of TWS observations are important on the perfor-
119 mance of the data assimilation process. In another effort, [van Dijk et al. \(2014\)](#) proposed an
120 alternative approach for estimating GRACE TWS errors in data assimilation. The triple collo-
121 cation technique was used to merge model-derived storage in (sub-) surface compartments with
122 TWS estimates from GRACE measurements ([van Dijk et al., 2014](#)). In the studies discussed
123 above, GRACE error covariance for different spatial resolutions is hardly treated. For example,
124 [Eicker et al. \(2014\)](#) considered error covariance of various spatial resolutions that were rescaled
125 (e.g., rescaling 0.5° to 5°) rather than solving for distinct spatial resolution individually (e.g.,
126 0.5° , 1° , and 5°).

127 In the present study, we extend the works above by employing a Local Analysis (LA) tech-
128 nique. LA allows utilization of different GRACE TWS spatial resolutions by addressing insta-
129 bility in data assimilation that arises from the GRACE covariance matrices of the corresponding
130 spatial resolutions. The contribution of this study is, therefore, twofold: (i) we mathematically
131 assess the efficiency of the localization technique to use GRACE TWS with its full error infor-
132 mation and with high spatial resolution in an assimilation framework; and (ii), we compare the
133 performance of a localization technique to in-situ data in a real case study covering the entire
134 Australian continent. These will assess the ability of local data assimilation in maximizing the
135 contribution of GRACE TWS into a hydrological model by considering its full error covariance
136 matrix. Here, we use the full variance-covariance of GRACE to establish the observation error
137 covariance matrices for the grid resolutions of 1° , 2° , 3° , 4° , 5° , and a basin scale, and examine
138 their effects on data assimilation. More importantly, for the first time, we offer a solution to
139 increase the performance of data assimilation in using GRACE data. A localization technique
140 is applied to account for correlations in high spatial resolution observations, which can lead to a
141 rank deficiency problem and correspondingly an instability in the data assimilation procedure.
142 In terms of localization technique, Local Analysis (LA) of the filter ([Evensen, 2003](#); [Ott et al.,](#)
143 [2004](#)) is considered mainly due to its ability in dealing with correlations by spatially limiting
144 the use of ensemble-based covariance information of high-dimensional systems to the limited

145 local region (Ott et al., 2004). LA effects on each data assimilation scenario (i.e., using different
146 spatial resolutions) are assessed to explore its ability for improving the results. In addition, the
147 application of LA has the potential to minimize a large part of error sources in the ensemble
148 filtering methods when a small number of ensembles is used (Mitchell and Houtekamer, 2000;
149 Houtekamer and Mitchell, 2001).

150 GRACE TWS data is assimilated into the World-Wide Water Resources Assessment (W3RA,
151 van Dijk, 2010) over Australia. The ensemble-based sequential technique of the Square Root
152 Analysis (SQRA) filtering scheme represented by Evensen (2004) is used to assimilate GRACE
153 TWS into W3RA. SQRA, which is a deterministic form of ensemble Kalman filtering, has
154 considerable advantages in comparison to some existing methods in terms of the computa-
155 tional speed, simplicity, and its independency to an observation perturbation unlike traditional
156 Kalman filtering methods (see detail in Section 3.1 and Khaki et al., 2017). In addition to im-
157 plementing the LA, in order to further address possible problems that arise from ensemble size,
158 sampling errors, and insufficient ensemble variance in ensemble-based techniques (Anderson et
159 al., 2007; Oke et al., 2007), ensemble inflation is applied. This technique, which has frequently
160 been used in previous works (e.g., Anderson and Anderson, 1999; Anderson et al., 2007; Ott
161 et al., 2004), tries to increase the variance of ensembles around the ensemble mean by inflating
162 prior ensembles (Anderson et al., 2007).

163 The remainder of this contribution is organized as follows: in Section 2, the GRACE
164 TWS data, W3RA, and in-situ observations are introduced. The SQRA filtering scheme used
165 for data assimilation, ensemble inflation, and the applied localization method are described in
166 Subsection 3.1 and details of an experiment set up are provided in Subsection 3.2. In Section
167 4, the results of data assimilation and their evaluation against the in-situ validation data are
168 presented and discussed, and finally in Section 5, the study is concluded.

169 2. Datasets

170 2.1. GRACE

171 Monthly GRACE level 2 (L2) potential coefficients products along with their full error
172 covariance information are obtained from the ITSG-Grace2014 gravity field model (Mayer-
173 Gürr et al., 2014). The solution is computed up to degree and order (d/o) 90 resulting in

174 approximately ~ 300 km spatial resolution at the equator. The study period (February 2003 to
175 December 2012) is limited by the availability of the climate data (see Section 2.2) to force the
176 hydrological model.

177 Following Swenson et al. (2008), degree 1 coefficients ([http://grace.jpl.nasa.gov/data/get-](http://grace.jpl.nasa.gov/data/get-data/geocenter/)
178 [data/geocenter/](http://grace.jpl.nasa.gov/data/get-data/geocenter/)) are replaced to account for the movement of the Earth's centre of mass. Degree
179 2 and order 0 (C_{20}) coefficients (<http://grace.jpl.nasa.gov/data/get-data/oblateness/>) are not
180 well determined and are replaced by those from Cheng and Tapley (2004). Correlated noise
181 in the TWS data products is reduced by applying de-stripping and smoothing using a Gaussian
182 averaging kernel with 300 km half radius following Swenson and Wahr (2006). This causes some
183 degree of signal attenuation (Klees et al., 2008) and moving anomalies from one region to another
184 (Chen et al., 2007). This leakage effect can lead to some degree of signal inference especially at
185 the land-ocean boundary. In order to address this issue, following Swenson and Wahr (2002), we
186 apply an isotropic kernel using a Lagrange multiplier filter to best balance signal and leakage
187 errors over the entire Australia. This filter uses a basin averaging kernel method expanded
188 in spherical harmonic coefficients and subsequently combined with L2 potential coefficients to
189 improve the GRACE estimates (see details in Swenson and Wahr, 2002).

190 The filtered gravity fields, are then converted to TWS changes (following Wahr and Mole-
191 naar, 1998) over the entire Australia in both grid and basin scales. The amount of rainfall over
192 Australia, especially over its northeast, western, and central parts, is low in comparison to other
193 inhabited continents on Earth leading to prolonged drought in the interior regions (Frootan
194 et al., 2016). This effect can be seen from the average precipitation (between February 2003
195 and December 2012) in Figure 1. This map shows small amount of rainfall over most parts
196 of Australia (e.g., the western and eastern parts). Therefore, an accurate estimation of water
197 storages (e.g., using hydrological models) is necessary to manage water resources in this region.
198 TWS changes from GRACE are gridded into the spatial grid resolutions of 1° , 2° , 3° , 4° , 5° ,
199 and also a basin scale for 12 major Australian drainage divisions and river basin (cf. Figure
200 1). As a number of studies have used basin averaged GRACE TWS for data assimilation (e.g.,
201 Zaitchik et al., 2008; Houborg et al., 2012), we test the LA in both grid and basin scales. Ac-
202 cordingly, for each grid size as well as basin scale error covariance matrices are calculated using
203 the full error information of the L2 potential coefficients for each month. Note that the errors
204 in lower degree potential coefficients provided along with degree 1 coefficients and C_{20} are sub-

205 stituted into the GRACE covariance matrix. No correlation is considered between the GRACE
206 covariance matrix and errors in the lower degree potential coefficients. This error information is
207 then used to reach observation errors for data assimilation. To this end, following [Schumacher](#)
208 [et al. \(2016\)](#), an error propagation is implemented to convert the full error information of the
209 GRACE coefficients to TWS errors.

FIGURE 1

210 2.2. W3RA

211 In this study, we use the World-Wide Water Resources Assessment system (W3RA),
212 which was developed in 2008 by the Commonwealth Scientific and Industrial Research Or-
213 ganisation (CSIRO) to monitor, represent and forecast Australia's terrestrial water cycles
214 (<http://www.wenfo.org/wald/data-software/>). W3RA is a grid distributed biophysical model
215 that simulates water stores and flows with significant information of water storages over Aus-
216 tralia ([van Dijk, 2010](#); [Renzullo et al., 2014](#)). Globally distributed $1^\circ \times 1^\circ$ minimum and max-
217 imum temperature, downwelling short-wave radiation, and precipitation from Princeton Uni-
218 versity (<http://hydrology.princeton.edu>) are used as meteorological forcing data (see detail in
219 [Sheffield et al., 2006](#)). The model parameters include effective soil parameters, water hold-
220 ing capacity and soil evaporation, relating greenness and groundwater recession, and saturated
221 area to catchment characteristics ([van Dijk et al., 2013](#)). Model state in this study includes the
222 W3RA water storages in the top, shallow, and deep root soil layers, groundwater storage, and
223 surface water storage in a one-dimensional system (vertical variability). Here, we use W3RA
224 (with a daily scale) for the same temporal coverage of GRACE (e.g., February 2003 to Decem-
225 ber 2012) and the spatial resolution of $1^\circ \times 1^\circ$. More detailed information on W3RA can be
226 found in [van Dijk et al. \(2013\)](#).

227 2.3. Validation Data

228 We use groundwater in-situ measurements over the Murray-Darling basin
229 extracted from the New South Wales Government (NSW) groundwater archive
230 (<http://waterinfo.nsw.gov.au/pinneena/gw.shtml>) to evaluate the performance of applied
231 data assimilation. Although data assimilation is done over entire Australia, due to limited

232 availability of in-situ stations, the existing in-situ measurements over the Murray-Darling basin
233 are used for result assessment. Measurements with data gaps and those that did not exhibit
234 seasonal variations are flagged as belonging to confined aquifers and are excluded (Houborg
235 et al., 2012; Tangdamrongsub et al., 2015). Therefore, daily and monthly well measurements
236 of 54 spatially distributed stations over the basin (cf. Figure 1) are used and time series
237 of groundwater storage anomalies are generated for each station. Selected well-water levels
238 need to be converted to variations in groundwater (GW) storage in terms of equivalent water
239 heights. This is usually done through the specification of yield estimates (e.g., Rodell et al.,
240 2007; Zaitchik et al., 2008). However, such information does not exist in this study. Hence,
241 following Tangdamrongsub et al. (2015), TWS variations from GRACE and soil moisture
242 products from Global Land Data Assimilation System (GLDAS) NOAH (Rodell et al., 2004)
243 are used to calculate the specific yield and scale the observed head water by modifying the
244 magnitude of GW time series (Tregoning et al., 2012). As Tregoning et al. (2012) showed,
245 the GW component can be extracted over Australia by removing the soil moisture component
246 from GRACE TWS data. Other water compartments including biomass and surface water
247 variations can be excluded due to their small contribution to regional scale mass variations
248 within Australia. Through this approach, rather than assuming a constant specific yield
249 everywhere (e.g., 0.1 by Tregoning et al., 2012), different yield values can be derived leading
250 to a more realistic representation of groundwater systems in different areas. The calculated
251 specific yields range between 0.08 and 0.16, falling within the 0.05–0.2 range suggested by
252 the Australian Bureau of Meteorology (BOM) and Seoane et al. (2013), hence justifying the
253 application of the method. The extracted yield factor is used at each in-situ location to scale
254 the observed in-situ head time series (see also Rodell et al., 2007; Longuevergne et al., 2013).
255 After removing temporal averages of in-situ groundwater time series, the anomaly time series
256 are used in this study to assess W3RA estimates after the assimilation process.

257 Further result assessment is done using in-situ soil moisture measurements. These datasets
258 are obtained from the moisture-monitoring network (<http://www.oznet.org.au/>) known as
259 OzNet network and spotted in the Murrumbidgee catchment (Smith et al., 2012). OzNet
260 network provides long-term records of measured volumetric soil moisture at various soil depths
261 at 57 locations across the Murrumbidgee catchment area (cf. Figure 1). The anomalies of
262 in-situ soil moisture measurements are calculated and then averaged into daily scale. Following
263 Renzullo et al. (2014), 0–8 cm data is used to evaluate the estimated model top-layer soil mois-

264 ture and the 0–30 cm and 0–90 cm measurements are applied for the evaluation of the model
 265 shallow root-zone soil moisture estimation.

266 3. Data Assimilation

267 3.1. Methods

268 3.1.1. Square Root Analysis (SQRA)

269 The solution of the data assimilation problem is based on Bayes' theorem (Jazwinski,
 270 1970; van Leeuwen et al., 1996), which tries to improve the model state by updating the prior
 271 Probability Density Function (PDF) whenever new observations are introduced. The sequential
 272 data assimilation technique solves the Bayesian estimation problem numerically by providing a
 273 probabilistic framework and sequentially estimates the whole system using propagated informa-
 274 tion (ensembles) only forward in time (Jardak et al., 2007). There are various filtering methods
 275 in this framework, however, one of the mostly applied techniques is ensemble-based Kalman
 276 filter. In this study, we use the square root analysis (SQRA) scheme for the Ensemble Kalman
 277 Filter (EnKF), represented by Evensen (2004) as a data assimilation filtering method. SQRA
 278 is a deterministic form of ensemble-based Kalman filters and uses a statistical sample of state
 279 estimates (Sakov et al., 2008). The model state contains N different vectors (N is the number
 280 of ensembles), each with the same size of the model state variables. The forecast model state
 281 is represented by $X^f = [X_1^f \dots X_N^f]$, where X_i^f ($i = 1 \dots N$) is the i th ensemble (hereafter
 282 'f' stands for forecast and 'a' stands for analysis). The model state forecast error covariance of
 283 P^f is defined by:

$$P^f = \frac{1}{N-1} \sum_{i=1}^N (X_i^f - \bar{X}^f)(X_i^f - \bar{X}^f)^T = \frac{1}{N-1} A^f A^{fT}, \quad (1)$$

284 where \bar{X}^f is the ensemble mean and can be calculated using,

$$\bar{X}^f = \frac{1}{N} \sum_{i=1}^N (X_i). \quad (2)$$

285 Forecast ensemble of anomalies, $A^f = [A_1^f \dots A_N^f]$, is the deviation of model state ensembles
 286 from the ensemble mean,

$$A_i^f = X_i^f - \bar{X}^f. \quad (3)$$

287 SQRA eliminates the need for the perturbation of measurements, which is essential in tradi-
 288 tional EnKF (Burgers et al., 1998). Instead, SQRA uses unperturbed observations without
 289 imposing any additional approximations like uncorrelated measurement errors (Evensen, 2004)
 290 by introducing a new sampling scheme. Rather than updating each sample separately in the
 291 analysis step, SQRA updates all of them in two stages; firstly by updating the ensemble-mean
 292 using \bar{X}^f (cf. Equation 1) as,

$$\bar{X}^a = \bar{X}^f + K(y - H\bar{X}^f), \quad i = 1 \dots N, \quad (4)$$

$$K = P^f(H)^T(HP^f(H)^T + R)^{-1}, \quad (5)$$

293 where \bar{X}^a is the mean analysis state, K represent the Kalman gain, y and R are the observation
 294 vector and associated covariance matrix. The transition matrix from the state vector space to
 295 the observation space is shown by H . Next, SQRA computes the ensemble anomalies. In this
 296 regard, one needs to first calculate the ensemble version of the analysis error covariance matrix,
 297 which can be done using Equation 6. Afterward, by inserting the forecast (P^f from Equation 1)
 298 and analysis (P^a from Equation 6) error covariances in Equation 7 and solving for A^a , analysis
 299 ensemble of anomaly can be computed.

$$P^a = \frac{A^a(A^a)^T}{N-1} \quad (6)$$

$$P^a = (I - KH)P^f \quad (7)$$

300 After a few simplification steps (cf. Evensen, 2004), A^a can be obtained by,

$$A^a = A^f V \sqrt{I - \Sigma^T \Sigma \Theta^T}, \quad (8)$$

301 where Σ and V are calculated using singular value decomposition of A^f ($A^f = U\Sigma V^T$). Γ
 302 refers to the singular value decomposition and Θ is a random orthogonal matrix (e.g., the right
 303 singular vectors from a singular value decomposition of a random $N \times N$ matrix) for ensemble
 304 redistribution of the variance reduction (cf. Evensen, 2004, 2007; Khaki et al., 2017).

305 3.1.2. Filter Tuning

306 Many studies have previously investigated the sensitivity of ensemble-based schemes
 307 on ensemble size (e.g., Houtekamer, 1995; Houtekamer and Mitchell, 1998; Keppenne, 2000;
 308 Mitchell et al., 2002; Keppenne and Rienecker, 2002). It has been proven that a large num-
 309 ber of ensemble members in ensemble data assimilation systems causes computation time to

310 significantly increase while using a small ensemble size can also be problematic, as it can lead
 311 to filter divergent or inaccurate estimation (Tippett et al., 2003). A successful ensemble-based
 312 filter needs to adequately span the model sub-space for a better approximation of probability
 313 distribution of the background errors (Ott et al., 2004). This, however, can be very challenging
 314 once a small ensemble number (considerably less than the model dimension) is used. To tackle
 315 this problem, we apply ensemble inflation, which uses a small coefficient to separately inflate
 316 prior ensemble deviation from the ensemble-mean and increases their variations (Anderson et
 317 al., 2007). Here, we use a constant factor ($S = 1.12$; Anderson, 2001) to inflate the ensemble
 318 perturbations as,

$$X'^f = S(X^f - \bar{X}^f) + \bar{X}^f, \quad (9)$$

319 with X'^f representing the new forecast state, which contains the inflated ensemble perturbation.

320 A further solution when dealing with a limited ensemble number is the application of lo-
 321 calization techniques initially proposed by Houtekamer and Mitchell (2001). In this study, we
 322 use the Local Analysis (LA) scheme not only to address the issue of the small ensemble num-
 323 ber, but also to investigate its effects in dealing with the GRACE error covariance for different
 324 spatial resolutions. LA works by restricting the information used for the covariance matrix
 325 computation to a spatially limited area and uses only measurements located within a certain
 326 distance from a grid point (Evensen, 2003; Ott et al., 2004; Khaki et al., 2017).

327 In using LA, at each horizontal grid point (m, n) , with m and n representing geographic
 328 latitude and longitude directions, respectively, the selected measurements close to the grid
 329 point contribute to the SQRA filtering process. This means that only particular state variables
 330 close to the point (m, n) within an assumed distance and corresponding observations at the
 331 same locations are used in the assimilation process. To do this, a local system state vector,
 332 observations, and their covariance matrix need to be chosen at each grid point separately.
 333 Following Ott et al. (2004), a model state vector $X(r)$ (r is a two-dimensional vector with r_{mn})
 334 is used to achieve the local forecast state vector X'^f_{mn} in Equation 9 using a linear operator
 335 M_{mn} by,

$$X'^f_{mn} = M_{mn}X'^f(r). \quad (10)$$

336 At the specific grid point of (m_0, n_0) , X'^f_{mn} contains the information of $X'^f(r_{m+m_0, n+n_0})$ with
 337 $-l \leq m - m_0, n - n_0 \leq l$ (l localization length) and limited to grid points close to (m_0, n_0)

338 within a $(2l + 1)$ by $(2l + 1)$ patch (Ott et al., 2004).

339 Local state vectors and observations within the local region (y_{mn}) with covariance matrix
340 R_{mn} can then be used in SQRA to locally estimate the model state for each grid point. In
341 case of using a gridded GRACE TWS dataset in a finer spatial resolution (e.g., 1° and 2°),
342 the calculated error covariances have rank deficiency mainly due to correlation errors (see more
343 details in Section 4.1). This problem can cause instability in the data assimilation procedure.
344 Applying LA, therefore, can be helpful since it numerically resolves the possible singularity
345 in the filtering process during data assimilation. Ott et al. (2004) proved that LA yields a
346 good approximate representation of the background covariance matrix using a small ensemble
347 number with a rank much lower than the state dimension. LA localization can also be used
348 in the vertical direction, where different water compartments (e.g., shallow and deep soil mois-
349 ture, groundwater storage, and surface water storage) exist. This can be helpful to vertically
350 decrease the influence of the layers on each other by limiting the filtering process to specific
351 layers, especially when there is a high correlation between the observed components at different
352 layers. Here, however, LA is applied only horizontally because the GRACE TWS observation
353 at each grid point is assimilated to an aggregate of water compartments at the same point.
354 Therefore, a vertical variability in system states is not reflected in the observation error covari-
355 ance. Furthermore, we are more interested in monitoring the performance of the localization
356 scheme on the GRACE covariance matrix rather than a state covariance matrix. Different trial
357 localisation lengths (2° to 10° for gridded TWSs) are applied in this study and their results are
358 assessed against independent groundwater in-situ measurements (cf. Section 2.3) to find the
359 best case (see details in Section 4.2).

360 3.2. Assimilating GRACE Data

361 In order to address the rather low temporal resolution of GRACE (approximately 30
362 days), its monthly data and errors are interpolated to 5-day data following Tangdamrongsub et
363 al. (2015), the spline interpolation between consecutive months is used to generate these time
364 series, which allows the ensemble to gradually change between updates. Next, the mean water
365 storage over the study area between 2003 and 2013 is calculated from the W3RA and is added
366 to GRACE TWS changes time series in order to achieve the absolute values. The provided
367 observations are assimilated into W3RA for the 5 different grid resolutions of 1° , 2° , 3° , 4° , and
368 5° and also in basin scales.

369 The $1^\circ \times 1^\circ$ spatial resolution of the model leads to a model state vector (X^f) with 794
 370 elements within the Australian continent. Each of these elements contains different water
 371 compartments. This means that the state vectors for every grid point in our experiments are
 372 composed of the different water storages, including top soil, shallow soil, and deep soil water,
 373 canopy, snow, surface, and groundwater. The observations matrix (H) accumulates the state
 374 variables (the individual water storages) at each grid point to determine the simulated TWS
 375 in order to update them with the GRACE TWS during assimilation. In the update steps, the
 376 5-day temporal average update increment (i.e., the difference between the simulated TWS and
 377 GRACE TWS) is applied.

378 Initial ensemble members are generated by perturbing the meteorological forcing fields fol-
 379 lowing [Renzullo et al. \(2014\)](#). In this regard, the three most important forcing variables includ-
 380 ing precipitation, temperature, and radiation and their reported error characteristics ([Sheffield
 381 et al., 2006](#)) are used. To generate the perturbations, we assume a multiplicative error of 30%
 382 for precipitation, an additive error of $50Wm^{-2}$ for the shortwave radiation, and an additive
 383 error of $2^\circ C$ for temperature ([Jones et al., 2007](#); [Renzullo et al., 2014](#)). Monte Carlo sam-
 384 pling of multivariate normal distributions with the errors representing the standard deviations
 385 without considering correlations (spatial and/or temporal) are used to produce an ensemble
 386 (according to [Renzullo et al., 2014](#)). Different ensemble sizes (30-120) and their spread are
 387 tested. The selected number of 72 members agrees with the suggestion by [Oke et al. \(2008\)](#) and
 388 shows promising performance and is used in this study. The perturbed meteorological forcing
 389 datasets, then, are integrated forward with the model for two years (January 2001 to January
 390 2003). This provided a set of state vectors at the beginning of the study period, considered as
 391 the initial ensemble. A schematic illustration of the assimilation process steps is provided in
 392 [Figure 2](#).

FIGURE 2

393 4. Results

394 In the following, we first analyze the effects of GRACE TWS spatial scaling on the
 395 error covariance matrix. Then, LA behavior in dealing with GRACE error covariance with
 396 different spatial resolutions is addressed. Afterwards, we evaluate the results of data assimilation

397 using LA with respect to different resolutions against the in-situ groundwater and soil moisture
 398 products. These results are also compared with the data assimilation process without applying
 399 LA (with a consideration of zero correlation in GRACE data) to be able to better investigate
 400 its effects on the model estimations.

401 *4.1. Scaling Effect*

402 In this section, we review the behavior of assimilating GRACE TWS data for different
 403 spatial resolutions into the W3RA model. To this end, GRACE TWS is assimilated with the
 404 following spatial resolutions, 1° , 2° , 3° , 4° , 5° , and a basin scale to monitor the effects of
 405 localization on the process. For each of the spatial resolution considered, 5-day GRACE TWS
 406 data (cf. Section 3.2) are assimilated into the model to address the coarser GRACE temporal
 407 scale in comparison to the model. As an example, in Figure 3, we compare the assimilated time
 408 series using the $1^\circ \times 1^\circ$ observations for a monthly (Figure 3a) and 5-day temporal scale over
 409 an arbitrary point (Figure 3c) to show the effect of temporal rescaling. The denser temporal
 410 resolution in Figure 3c eventuates in a much smoother time series. This is more obvious in
 411 Figures 3b and 3d, which show only one year of the time series, respectively presented in Figures
 412 3a and 3c. Given daily time steps of W3RA, assimilating GRACE TWS data once a month
 413 (e.g., in the middle of the month) causes unnatural jumps at the assimilation steps (cf. Figure
 414 3b). Such a jump is much smaller in magnitude in Figure 3d where a 5-day sampling interval
 415 is used. This leads to keeping the ensemble spread smoother without significant artifacts or
 416 temporal discontinuities. It should be mentioned that another solution for keeping ensemble
 417 spread smooth is the application of ensemble Kalman smoother (EnKS), which redistributes
 418 analysis increments evenly over all days of the month with the expense of more computational
 419 cost (see, e.g., Zaitchik et al., 2008; Houborg et al., 2012).

FIGURE 3

420 We can now assess the behaviour of LA on data assimilation when the full error covari-
 421 ance of GRACE is used for the different applied spatial scales. Figure 4 shows the estimated
 422 correlation matrices for each grid resolution (following Eicker et al., 2014). This figure helps
 423 in understanding how different grid resolutions affect the corresponding observation covariance
 424 matrix. It can be seen that the spatial scaling influences the correlation between points. The

425 correlation (off-diagonal elements) between grid points decreases for larger grid resolutions, with
 426 the least for the 5° gridded TWSs, which is significantly less than that of 1° grid resolution.
 427 This correlation is even smaller when the basin scale GRACE data is considered. To clarify how
 428 this affects the data assimilation procedure, Table 1 indicates the number of gridded observa-
 429 tions in various grid resolutions and the estimated ranks of covariance matrices. We find that
 430 there is a close relationship between the grid resolution and covariance matrix rank (cf. Table
 431 1). As mentioned earlier, rank deficiency problem in covariance matrices causes instability in
 432 the data assimilation procedure and inaccurate estimations. The application of LA, however,
 433 numerically addresses this issue. It can be seen that LA affects the estimated covariance matrix
 434 rank for each grid resolution. Details on the number of observations and the rank of the re-
 435 spective covariance matrices (cf. Table 1) demonstrates the LA effect on improving the process
 436 by solving the mathematical problem related to the rank deficiency especially in the cases of 1°
 437 and 2°.

438 FIGURE 4

TABLE 1

439 Rank deficiency likely happens for error covariance matrices of GRACE TWS with grid
 440 resolutions that GRACE can resolve (e.g., 3° or coarser). However, when using smaller grid
 441 resolutions, the matrix does not have a full rank leading to instabilities in the data assimilation
 442 procedure. Although applying GRACE data at lower spatial resolutions might be helpful in
 443 dealing with the covariance matrix, this will reduce the number of observations during data
 444 assimilation process (cf. Table 1) leading to some loss of signal in the observations. This might
 445 not be obvious considering the spatial correlation between grid points for higher resolution
 446 GRACE TWS. However, we show that using more observations and considering their full error
 447 covariance information in the assimilation process allows more information to be transferred
 448 with a higher number of observations into the system states. In this regard, we use the frequently
 449 employed indexes of Shannon Information Content (SIC or entropy reduction) and degrees of
 450 freedom (Dof) to measure information, which is transferred from observations into the system
 451 states (Rodgers, 2000) at the assimilation steps. SIC ($\frac{1}{2}\ln(P^f/P^a)$) uses the information in
 452 the state probability density function (pdf) before and after assimilation to reflect a real-valued
 453 functional (Shannon and Weaver, 1949). Dof ($n - \text{trace}(P^a/P^f)$), with n number of observations)

454 on the other hand, is a measure of the amount of information from observations that is used
 455 (Stewart et al., 2008). For each grid resolution, the indexes of SIC and Dof are measured
 456 (Figure 5).

FIGURE 5

457 It can be seen in Figure 5 that by decreasing the spatial resolution, some information
 458 contained within the observations is lost. Therefore, although increasing the scale size (reducing
 459 the resolution) might be helpful in dealing with GRACE error covariance, it is at the cost of
 460 losing part of the signal. This justifies the application of LA, which allows us to use information
 461 with a higher spatial resolution in datasets.

462 As outlined in section 3.1.2, one important effect of LA is underestimating the influences of
 463 spatially distant grid points on each other. The distance in localization preserves the informa-
 464 tion in observations close to each other while at the same time making it possible to use full
 465 error covariance information. To demonstrate this, we consider the correlation coefficient of the
 466 arbitrary point (at a location 136.6854°E and 23.9015°S) to the other grid points in Figure 6.
 467 This point is chosen to be approximately in the middle of the study area for a better visual
 468 representation while similar results are achieved for all other grid points. We integrate the
 469 model and performed data assimilation using the 1° GRACE TWS (as the worst case among
 470 different applied resolutions) during the study period. The average correlation coefficients be-
 471 tween the arbitrary point and the other grid points before and after assimilation using LA are
 472 then measured. Figure 6b shows how LA successfully reduces the correlation coefficients for
 473 more distant grid elements but maintains the correlations in the close vicinity.

FIGURE 6

474 The important point to consider when using LA is the removal of some information from the
 475 data, which is not desirable. Thus, attention needs to be taken when choosing the localization
 476 length to preserve the adequate continuity of analysis on adjacent points (Zeng, 2014). LA
 477 length depends on the observation density and can be chosen arbitrarily. After testing different
 478 localization lengths, it is found that a small length (e.g., less than 5° for $1^{\circ}\times 1^{\circ}$ GRACE TWS)
 479 can result in large errors even though there would be no inverse problem in assimilation filter.

480 We use groundwater in-situ measurements to assess the results of applying different localiza-
 481 tion lengths (2° to 10° for gridded TWSs). For every scenario (different grid resolutions), we
 482 interpolate assimilation time series at the location of the groundwater in-situ and calculate
 483 the root-mean-square error (RMSE). The average computed RMSE of each grid resolution for
 484 the applied lengths (Figure 7) show that better results are obtained using the 5° localization
 485 halfwidth length compared to the other applied localization lengths.

FIGURE 7

486 A similar experiment is implemented to find efficient localization length for a basin scale
 487 spatial resolution. For each basin, we test different lengths mostly larger than those for grid
 488 scales (e.g., 5° to 15° with the best performance of 10° radii in average) and estimate TWS
 489 errors using the GRACE TWS data where in-situ measurements are not available for all basins.
 490 The localization length with the least error for each basin (Figure 8) is used to assess the LA
 491 effects at the basin scale and also to compare corresponding results with grid scale resolutions.

FIGURE 8

492 4.2. Assessment with in-situ data

493 Post processed in-situ measurements of groundwater changes (cf. Section 2.3) over the
 494 Murray-Darling basin as well as OzNet soil moisture network in the Murrumbidgee catchment
 495 (see Figure 1 for the location of the catchment) are used to evaluate the assimilation results.
 496 First, to compare the time series obtained from assimilation results with those of in-situ mea-
 497 surements, the GW results for each spatial resolution considered are spatially interpolated using
 498 the nearest neighbor (the closest four data values) to the location of the in-situ measurements.
 499 Afterward, the error time series are computed as the difference between the estimated GW and
 500 in-situ GW measurements. We then estimate average errors using these time series for each
 501 scenario of data assimilation.

502 The TWS time series of the assimilation process for the case of 3° is shown in Figure 9a.
 503 Data assimilation with this spatial resolution results in a minimum GW error compared to the
 504 in-situ measurements. This figure also contains the open loop time series which refers to the
 505 estimations without implementation of any data assimilation and the assimilated observations.

506 The absolute errors, i.e., the difference between the in-situ measurements and either the open
 507 loop or the assimilated estimates (for the best case of 3° spatial resolution) are presented in
 508 Figure 9b. The assimilated time series fits well with the groundwater in-situ measurements (cf.
 509 Figure 9a) and results in a higher correlation than the open loop time series (85% average).
 510 Note that in terms of representing the hydrology, sometimes the estimates do not really depict
 511 the signal of the in-situ measurements. In some instances, the error (for no assimilation) is
 512 as large as the signal itself. This could be due to the fact that W3RA only simulates the dy-
 513 namics of unconfined aquifers, that is, groundwater that receives soil drainage and discharges
 514 into streams. In some cases, a deeper (confined) aquifer underneath can also affect ground-
 515 water measurements. Nevertheless, data assimilation causes the updated time series to reflect
 516 better the real fluctuations in groundwater storage in most of the cases as given by the in-situ
 517 measurements.

FIGURE 9

518 The average estimated error of all GW in-situ stations during the study period for each
 519 scenario illustrates the LA performances for the different spatial resolutions (Figure 10). The
 520 least error is obtained from the 3° spatial resolution by comparing assimilation results of all
 521 scenarios. In addition, to be able to monitor the effectiveness of LA, data assimilation is also
 522 applied using GRACE-derived TWS and only diagonal elements of its error covariance matrix.
 523 Results without applying LA (represented in Figure 10) refers to this case where correlations
 524 between grid points are neglected. This comparison is of interest because many of the previously
 525 presented studies in using GRACE for hydrological data assimilation have neglected the existing
 526 correlation in observations (see e.g., [Zaitchik et al., 2008](#); [Houborg et al., 2012](#); [Li et al., 2012](#);
 527 [Tangdamrongsub et al., 2015](#); [Sun et al., 2015](#); [Kumar et al., 2016](#)).

FIGURE 10

528 It can be seen that locally applying the GRACE observations effectively reduces errors for
 529 every grid resolution considered in comparison to the uncorrelated observation assumption.
 530 This, however, is more obvious for higher spatial resolution (e.g., 3° and higher) where a large
 531 difference between the assimilation results with and without the application of LA can be found.
 532 Although LA mathematically solves the inverse problem for using 1° gridded GRACE TWS

533 data and associated error covariance (cf. Table 1) in the filtering process, this spatial resolution
534 results in a larger error in comparison to the other scenarios. From Section 2.1, we know that
535 truncating and smoothing procedures cause losing a part of GRACE data, especially in higher
536 frequencies. Rescaling such a data into 1° spatial resolution results in an error in gridded
537 GRACE TWS and correspondingly in the assimilation result (cf. Figure 10). Figure 10 shows
538 that increasing the spatial resolution results in a better estimation when LA is not applied.
539 This error reduction by using a higher spatial resolution is also true when LA is applied but
540 only to the point of 3° . After this point, errors start increasing, which can be explained by
541 fewer observations used leading to less information content to be transferred to model states.
542 The application of LA, however, reduces the error for all spatial resolutions while in an absolute
543 sense, the smallest errors are obtained for 3° . Interestingly, this spatial resolution is about the
544 spatial resolution that GRACE can resolve.

545 More detailed results are proposed in Figure 11 and Table 2 in terms of RMSE and cor-
546 relation analysis. As mentioned before, first, assimilation time series are interpolated at the
547 location of the groundwater in-situs and then, their anomalies are calculated. A similar proce-
548 dure is also applied to achieve assimilation time series over the soil moisture in-situ stations.
549 Then for all stations, RMSE and correlation factor between assimilation results (for various
550 scenarios) and in-situ measurements are calculated and their averages are used for assessment.
551 Note that considering the difference between W3RA estimations (column water storage) and
552 the OzNet measurements (volumetric soil moisture), only correlation analysis is assumed for
553 assessing results against soil moisture in-situ data. The reason for this refers to the fact that
554 converting model outputs (with unit 'mm') into volumetric units may introduce a bias (Ren-
555 zullo et al., 2014). Estimated correlations between assimilation results and OzNet soil moisture
556 (an average correlation for the total soil column; Figure 11a) as well as groundwater in-situ
557 level data (Figure 11b) demonstrate the ability of LA in dealing with GRACE data. Also, both
558 correlation analyses show that applying GRACE TWS with 3° leads to closer results to the
559 in-situ measurements.

560 FIGURE 11

TABLE 2

561 Based on the results in Table 2, all the results successfully improved the model estimation

562 of water storage variation. Applying LA in data assimilation leads up to 24.73% (13% average)
563 better estimations in comparison to the non-correlated assumption. This proves the importance
564 of using local data assimilation for incorporating GRACE data into the hydrological model. We
565 know from Eicker et al. (2014) that spatial upscaling of GRACE data to coarser resolutions
566 (e.g., 5°) can significantly stabilize the assimilation process leading to more reliable results,
567 however, LA can improve the results not only for these resolutions but also for smaller grid
568 sizes (cf. Table 2).

569 It can be seen from Table 2 that using gridded TWS observation with 3° shows the best
570 performance in terms of RMSE. Although there is no rank deficiency in using the full error
571 covariance matrix for this grid resolution, local implementation of the assimilation process
572 helps to improve the agreement with the in-situ measurements. The reason why LA does not
573 have a similar impact on finer spatial resolutions, especially for a 1° resolution in comparison
574 to 3° , could be due to the characteristic of GRACE L2 product as a degree limited data,
575 e.g., truncated spherical harmonics sets. An interesting observation from Table 2 refers to the
576 results of using GRACE TWS for a 2° spatial resolution. Considering Table 1, employing the
577 2° grid resolution causes a rank deficiency in covariance matrix leading to the unstable data
578 assimilation. LA successfully solves this problem and significantly improves the results with a
579 better performance (57.87% improvement). Fewer observations incorporated in the assimilation
580 on a basin scale and for 5° resolution in comparison to the other spatial scales (e.g., 3°) leads
581 to a weaker performance for these two cases.

582 5. Conclusion

583 The global time variable terrestrial water storage (TWS) data from the Gravity Recovery
584 And Climate Experiment (GRACE) has provide an important opportunity for a hydrological
585 model adjustment. In this study, we assessed the performance of local analysis (LA) method
586 in accounting for the existing correlation in GRACE data and improving its effect on model
587 states. To this end, we assimilated the GRACE-derived TWS changes into the World-Wide
588 Water Resources Assessment system (W3RA) during 2003 to 2012 using Square Root Analysis
589 (SQRA) filtering technique. LA was applied to (i) solve the mathematical problem of using
590 correlated data for assimilation especially when the observation spatial resolution is high (e.g., 1°
591 gridded TWS), and (ii) improve the assimilation results using GRACE TWS data for different

592 spatial resolutions (1° to 5° and a basin scale). The observations were applied for a 5-day
593 temporal scale and for 5 different grid resolutions to monitor the impact of LA on each scenario.
594 The results showed that implementing LA successfully reduced data assimilation errors for all
595 the cases (54.08% on average). This improvement is larger for the cases with smaller grid
596 sizes along with the higher error correlations. LA addressed the rank deficiency problem in
597 using the full information from the error covariance matrix for a higher spatial resolution of
598 GRACE TWS data (e.g., 1°). This, to the best of our knowledge, for the first time, allowed
599 us to be able to apply GRACE TWS considering spatial error correlation information at finer
600 spatial resolutions (e.g., 1° and 2°) for the hydrological data assimilation. LA also improved the
601 assimilation results at all grid resolutions and basin scale especially in comparison to using non-
602 correlated observations (13.76% average). This highlights the great potential of LA in different
603 scenarios for improved data assimilation. The best performance with 67.84% improvement was
604 found with the application of GRACE data in assimilation with 3° spatial resolution. Overall,
605 the importance of the application of LA in hydrological data assimilation is: (1) stabilising
606 the assimilation of GRACE TWS observation using its full error covariance for finer spatial
607 resolutions (e.g., 1° and 2°), and (2) improving the results for all the spatial grid sizes without
608 the assumption of white noise. This study offered a method to deal with the GRACE error
609 covariance matrix during data assimilation, however, further assessment needs to be undertaken
610 to examine other potential methods like inflation of the observation error variances and circulant
611 approximation.

612 **Acknowledgement**

613 We would like to thank professor Harrie-Jan Hendricks-Franssen, the associate editor
614 of *Advances in Water Resources*, and Dr. Manuela Girotto for their useful comments, which
615 contributed to the improvement of this study. M. Khaki is grateful for the research grant of
616 Curtin International Postgraduate Research Scholarships (CIPRS)/ORD Scholarship provided
617 by Curtin University (Australia). This work is a TIGeR publication.

618 **References**619 **References**

- 620 Alsdorf, D.E., Rodriguez, E., Lettenmaier, D.P., 2007. Measuring surface water from space.
621 *Rev. Geophys.*, 45, RG2002, doi:10.1029/2006RG000197.
- 622 Anderson, J.L., Anderson, S.L., 1999. A Monte Carlo implementation of the nonlinear filtering
623 problem to produce ensemble assimilations and forecasts. *Mon Weather Rev* 127:27412758.
- 624 Anderson, J., 2001. An Ensemble Adjustment Kalman Filter for Data As-
625 simulation. *Mon. Wea. Rev.*, 129, 28842903, [http://dx.doi.org/10.1175/1520-0493\(2001\)129;2884:AEAKFF;2.0.CO;2](http://dx.doi.org/10.1175/1520-0493(2001)129;2884:AEAKFF;2.0.CO;2).
- 627 Anderson, M.C., Norman, J.M., Mecikalski, J.R., Otkin, J.A., Kustas, W.P., 2007. A climato-
628 logical study of evapotranspiration and moisture stress across the continental United States
629 based on thermal remote sensing: 1. Model formulation. *J. Geophys. Res.* 112 (D10117).
630 <http://dx.doi.org/10.1029/2006JD007506>.
- 631 Bennett, A. F., 2002. *Inverse Modeling of the Ocean and Atmosphere*. 234 pp., Cambridge
632 Univ. Press, New York.
- 633 Bergemann, K., Reich, S., 2010. A localization technique for ensemble Kalman filters. *Q. J. R.*
634 *Meteorol. Soc.* 136: 701707.
- 635 Berger, H., Forsythe, M., 2004. Satellite wind superobbing. Met Office Forecasting Research
636 Technical Report, 451.
- 637 Bertino, L., Evensen G., Wackernagel, H., 2003. Sequential Data Assimilation Techniques in
638 Oceanography. *International Statistical Review*, Vol. 71, No. 2, pp. 223-241.
- 639 Brocca, L., Melone, F., Moramarco, T., Wagner, W., Naeimi, V., Bartalis, Z., Hasenauer,
640 S., 2010. Improving runoff prediction through the assimilation of the ASCAT soil moisture
641 product, *Hydrol. Earth Syst. Sci.*, 14, 18811893, [http://dx.doi.org/10.5194/hess-14-1881-](http://dx.doi.org/10.5194/hess-14-1881-2010)
642 2010.
- 643 Burgers, G., van Leeuwen, P.J., Evensen, G., 1998. Analysis scheme in the ensemble Kalman
644 filter, *Mon. Wea. Rev.*, 126, 17191724.

- 645 Chen, J.L., Wilson, C.R., Famiglietti, J.S., Rodell, M., 2007. Attenuation effect on seasonal
646 basin-scale water storage changes from GRACE time-variable gravity. *Journal of Geodesy*,
647 81, 4, 237245. <http://dx.doi.org/10.1007/s00190-006-0104-2>.
- 648 Chen, J.L., Wilson, C.R., Tapley, B.D., 2013. Contribution of ice sheet and mountain glacier
649 melt to recent sea level rise. *Nat. Geosci.*, 6, 549552, <http://dx.doi.org/10.1038/ngeo1829>.
- 650 Cheng, M.K., Tapley, B.D., 2004. Variations in the Earth's oblateness during
651 the past 28 years. *Journal of Geophysical Research, Solid Earth*, 109, B09402.
652 <http://dx.doi.org/10.1029/2004JB003028>.
- 653 Clark, M.P., Rupp, D.E., Woods, R.A., Zheng, X., Ibbitt, R.P., Slater, A.G., 2008. Data
654 assimilative modeling investigation of Gulf Stream Warm Core Ring interaction with
655 continental shelf and slope circulation, Hydrological data assimilation with the ensem-
656 ble Kalman filter: Use of streamflow observations to update states in a distributed
657 hydrological model. *Advances in Water Resources*, 31, 10, 1309-1324, ISSN 0309-1708,
658 <http://dx.doi.org/10.1016/j.advwatres.2008.06.005>.
- 659 Coumou, D., Rahmstorf, S., 2012. A decade of weather extremes. *Nature Clim. Change*, 2(7),
660 491-496.
- 661 Crow, W., Wood, E., 2003. The assimilation of remotely sensed soil brightness temperature
662 imagery into a land surface model using ensemble filtering: A case study based on ESTAR
663 measurements during SGP97. *Adv. Water Res.*, 26, 137149.
- 664 Dando, M. L., Thorpe, A. J., Eyre, J. R., 2007. The optimal density of atmospheric sounder
665 observations in the Met Office NWP system. *Q.J.R.Meteorol.Soc.*, 133:19331943.
- 666 Eicker, A., Schumacher, M., Kusche, J., Dll, P., Mller-Schmied, H., 2014. Calibration/data
667 assimilation approach for integrating GRACE data into the WaterGAP global hydrology
668 model (WGHM) using an ensemble Kalman filter: first results. *SurvGeophys*, 35(6):12851309.
669 <http://dx.doi.org/10.1007/s10712-014-9309-8>.
- 670 Elbern, H., Schmidt, H., 2001. Ozone episode analysis by fourdimensional variational chemistry
671 data assimilation. *J. Geophys. Res.*, 106, 35693590.
- 672 Evensen, G., 2003. The ensemble Kalman filter: Theoretical formulation and practical imple-
673 mentation. *Ocean Dynamics*, 53, 343367, <http://dx.doi.org/10.1007/s10236-003-0036-9>.

- 674 Evensen, G., 2004. Sampling strategies and square root analysis schemes for the EnKF. *Ocean*
675 *Dyn.* 54(6), 539-560.
- 676 Evensen, G., 2007. *Data Assimilation: The Ensemble Kalman Filter*. Springer, 279 pp.
- 677 Famiglietti, J.S., Rodell, M., 2013. Water in the balance. *Science*, 340, 6138, 1300-1301.
678 <http://dx.doi.org/10.1126/science.1236460>.
- 679 Forootan, E., Rietbroek, R., Kusche, J., Sharifi, M.A., Awange, J., Schmidt, M., Omondi, P.,
680 Famiglietti, J., 2014. Separation of large scale water storage patterns over Iran using GRACE,
681 altimetry and hydrological data. *Journal of Remote Sensing of Environment*, 140, 580-595.
682 <http://doi.org/10.1016/j.jrse.2013.09.025>
- 683 Forootan, E., Khandu, Awange, J., Schumacher, M., Anyah, R., van Dijk, A., Kusche, J.,
684 2016. Quantifying the impacts of ENSO and IOD on rain gauge and remotely sensed
685 precipitation products over Australia. *Remote Sensing of Environment*, 172, Pages 50-66,
686 <http://dx.doi.org/10.1016/j.jrse.2015.10.027>.
- 687 Garner, T.W., Wolf, R.A., Spiro, R.W., Thomsen, M.F., 1999. First attempt at assimilating
688 data to constrain a magnetospheric model. *J. Geophys. Res.*, 104(A11), 25145-25152,
689 <http://dx.doi.org/10.1029/1999JA900274>.
- 690 Giroto, M., De Lannoy, G.J., Reichle, R.H., Rodell, M. 2016. Assimilation of gridded terres-
691 trial water storage observations from GRACE into a land surface model. *Water Resources*
692 *Research*, 52(5), 4164-4183.
- 693 Giroto, M., De Lannoy, G.J., Reichle, R.H., Rodell, M., Draper, C., Bhanja, S.N., Mukherjee,
694 A. 2017. Benefits and Pitfalls of GRACE Data Assimilation: a Case Study of Terrestrial
695 Water Storage Depletion in India. *Geophysical Research Letters*.
- 696 Giustarini, L., Matgen, P., Hostache, R., Montanari, M., Plaza, D., Pauwels, V.R.N., De Lan-
697 noy, G.J.M., De Keyser, R., Pfister, L., Hoffmann, L., Savenije, H.H.G., 2011. Assimilating
698 SAR-derived water level data into a hydraulic model: a case study. *Hydrol. Earth Syst. Sci.*,
699 15, 2349-2365, <http://dx.doi.org/10.5194/hess-15-2349-2011>.
- 700 Hamill, T.M., Snyder, C. (2002); Using improved background-error covariances from
701 an ensemble Kalman filter for adaptive observations. *Mon Wea Rev* 130:1552-1572.
702 [http://dx.doi.org/10.1175/1520-0493\(2002\)130<1552:UIBECF>2.0.CO;2](http://dx.doi.org/10.1175/1520-0493(2002)130<1552:UIBECF>2.0.CO;2).

- 703 Hoteit, I., Luo, X., Pham, D.T., 2012. Particle Kalman Filtering: A Nonlinear Bayesian Frame-
704 work for Ensemble Kalman Filters. *Monthly Weather Review*, 140:2, 528-542.
- 705 Houborg, R., Rodell, M., Li, B., Reichle, R.H., Zaitchik, B.F., 2012. Drought
706 indicators based on model-assimilated Gravity Recovery and Climate Experiment
707 (GRACE) terrestrial water storage observations. *Water Resour Res* 48:W07525.
708 <http://dx.doi.org/10.1029/2011WR011291>.
- 709 Houtekamer, P.L., 1995. The construction of optimal perturbations. *Mon Weather Rev*
710 123:28882898.
- 711 Houtekamer, P.L., Mitchell, H.L., 1998. Data assimilation using an ensemble Kalman filter
712 technique. *Mon. Wea. Rev.*, 126, 796 811.
- 713 Houtekamer, P.L., Mitchell, H.L., 2001. A Sequential Ensemble Kalman Filter for Atmospheric
714 Data Assimilation. *Mon. Wea. Rev.*, 129:1, 123-137.
- 715 Huffman, G., Bolvin, D., 2012. TRMM and other data precipitation data set documentation.
716 Mesoscale Atmospheric Processes Laboratory, NASA Goddard Space Flight Center and Sci-
717 ence Systems and Applications, Inc.
- 718 Huntington, T.G., 2006. Evidence for intensification of the global water cycle: Review and
719 synthesis. *J. Hydrol.*, 319(14), 8395.
- 720 Jardak, M., Navon, I.M., Zupanski, M., 2007. Comparison of sequential data assimilation meth-
721 ods for the Kuramoto-Sivashinsky equation. *International journal for numerical methods in*
722 *fluids*, Volume 62, Issue 4, 374402, <http://dx.doi.org/10.1002/fd.2020>.
- 723 Jazwinski, A.H., 1970. *Stochastic Processes and Filtering Theory*. Academic Press, 376 pp.
- 724 Jones, D.A., Wang, W., Fawcett, R., Grant, I., 2007. Climate data for the Australian water
725 availability project. In: *Australian Water Availability Project Milestone Report*. Bur. Met.,
726 Australia, 37pp.
- 727 Kalnay, E., 2003. *Atmospheric modelling, data assimilation and predictability*. Cam-
728 bridge University Press. pp. xxii 341. ISBNs 0 521 79179 0, 0 521 79629 6.
729 <http://dx.doi.org/10.1256/00359000360683511>.

- 730 Keppenne, C.L., 2000. Data assimilation into a primitive-equation model with a parallel en-
731 semble Kalman filter. *Mon Weather Rev* 128:19711981.
- 732 Keppenne, C.L., Rienecker, M., 2002. Initial testing of a massively parallel ensemble Kalman
733 filter with the poseidon isopycnal ocean general circulation model. *Mon Weather Rev*
734 130:29512965.
- 735 Khaki, M., Hoteit, I., Kuhn, M., Awange, J., Forootan, E., van Dijk, A.I.J.M., Schumacher,
736 M., Pattiaratchi, C., 2017. Assessing sequential data assimilation techniques for integrating
737 GRACE data into a hydrological model, *Advances in Water Resources*, Volume 107, Pages
738 301-316, ISSN 0309-1708, <http://dx.doi.org/10.1016/j.advwatres.2017.07.001>.
- 739 Klees, R., Revtova, E.A., Gunter, B.C., Ditmar, P., Oudman, E., Winsemius, H.C., 2008.
740 The design of an optimal filter for monthly GRACE gravity models. *Geophysical Journal*
741 *International*, 175, 2, 417-432, <http://dx.doi.org/10.1111/j.1365-246X.2008.03922.x>.
- 742 Kumar, S.V., Peters-Lidard, C.D., Mocko, D., Reichle, R.H., Liu, Y., Arsenault, K.R., Xia,
743 Y., Ek, M., Riggs, G., Livneh, B., Cosh, M., 2014. Assimilation of remotely sensed soil
744 moisture and snow depth retrievals for drought estimation, *Journal of Hydrometeorology*, 15,
745 2446-2469, <http://dx.doi.org/10.1175/JHM-D-13-0132.1>.
- 746 Kumar, S.V., Peters-Lidard, C.D., Santanello, J.A., Reichle, R.H., Draper, C.S., Koster,
747 R.D., Nearing, G., Jasinski, M.F., 2015. Evaluating the utility of satellite soil mois-
748 ture retrievals over irrigated areas and the ability of land data assimilation methods to
749 correct for unmodeled processes, *Hydrology and Earth System Sciences*, 19, 4463-4478,
750 <http://dx.doi.org/10.5194/hess-19-4463-2015>.
- 751 Kumar, S., Zaitchik, B., Peters-Lidard, C., Rodell, M., Reichle, R., Li, B., Jasinski, M.,
752 Mocko, D., 2016. Assimilation of Gridded GRACE Terrestrial Water Storage Estimates
753 in the North American Land Data Assimilation System. *J. Hydrometeor.*, 17, 19511972,
754 <http://dx.doi.org/10.1175/JHM-D-15-0157.1>.
- 755 Kusche, J., 2007. Approximate decorrelation and non-isotropic smoothing of time-variable
756 GRACE-type gravity field models. *J. Geod.*, 81, 733739.
- 757 Kusche, J., Klemann, V., Bosch, W., 2012. Mass distribution and mass transport in the Earth
758 system. *Journal of Geodynamics*, 59-60, 1-8. <http://doi.org/10.1016/j.jog.2012.03.003>.

- 759 Lahoz, W.A., Geer, A.J., Bekki, S., Bormann, N., Ceccherini, S., Elbern, H., Errera, Q., Eskes,
760 H.J., Fonteyn, D., Jackson, D.R., Khattatov, B., 2007. The Assimilation of Envisat data
761 (ASSET) project. *Atmos. Chem. Phys.*, 7, 1773 - 1796.
- 762 Li, B., Rodell, M., Zaitchik, B.F., Reichle, R.H., Koster, R.D., van Dam, T.M., 2012. As-
763 simulation of GRACE terrestrial water storage into a land surface model: Evaluation and
764 potential value for drought monitoring in western and central Europe. *Journal of Hydrology*,
765 <http://dx.doi.org/10.1016/j.jhydrol.2012.04.035>.
- 766 Liu, Z.Q., Rabier, F., 2003. The potential of high-density observations for numerical weather
767 prediction: A study with simulated observations. *Q.J.R.Meteorol.Soc.*, 129, 30133035.
- 768 Liu, Y., Weerts, A.H., Clark, M., Hendricks Franssen, H.-J., Kumar, S., Moradkhani, H., Seo,
769 D.-J., Schwanenberg, D., Smith, P., van Dijk, A.I.J.M., van Velzen, N., He, M., Lee, H.,
770 Noh, S.J., Rakovec, O., and Restrepo, P., 2012. Advancing data assimilation in operational
771 hydrologic forecasting: progresses, challenges, and emerging opportunities. *Hydrol. Earth*
772 *Syst. Sci.*, 16, 3863-3887, <http://dx.doi.org/10.5194/hess-16-3863-2012>.
- 773 Liu, Y., Peters-Lidard, C.D., Kumar, S., Foster, J.L., Shaw, M., Tian, Y., Fall, G.M., 2013. As-
774 simulating satellitebased snow depth and snow cover products for improving snow predictions
775 in Alaska, *Adv. Water Res.*, 54, 208227, <http://dx.doi.org/10.1016/j.advwatres.2013.02.005>.
- 776 Longuevergne, L., Scanlon, B.R., Wilson, C.R., 2010. GRACE Hydrological estimates for small
777 basins: Evaluating processing approaches on the High Plains Aquifer, USA. *Water Resources*
778 *Research*, 46, 11, W11517. <http://dx.doi.org/10.1029/2009WR008564>.
- 779 Longuevergne, L., Wilson, C.R., Scanlon, B.R., Crtaux, J.F., 2013. GRACE water storage
780 estimates for the Middle East and other regions with significant reservoir and lake storage.
781 *Hydrol. Earth Syst. Sci.*, 17, 48174830, <http://dx.doi.org/10.5194/hess-17-4817-2013>.
- 782 Mayer-Gürr, T., Zehentner, N., Klinger, B., Kvas, A., 2014. ITSG-Grace2014: a new GRACE
783 gravity field release computed in Graz. - in: GRACE Science Team Meeting (GSTM). Pots-
784 dam am: 29.09.2014.
- 785 Mitchell, H.L., Houtekamer, P.L., 2000. An adaptive ensemble Kalman filter. *Mon. Wea. Rev.*
786 128, 416433.

- 787 Mitchell, H.L., Houtekamer, P.L., Pellerin, G., 2002. Ensemble size, balance, and model-error
788 representation in an ensemble Kalman filter. *Mon Weather Rev* 130:27912808.
- 789 Moradkhani, H., Hsu, K., Hong, Y., Sorooshian, S., 2006. Investigating the impact of remotely
790 sensed precipitation and hydrologic model uncertainties on the ensemble streamflow forecast-
791 ing. *Geophys. Res. Lett.* 33, L12107.
- 792 Munier, S., Aires, F., Schlaffe, S., Prigent, C., Papa, F., Maisongrande, P., Pan, M., 2014.
793 Combining data sets of satellite-retrieved products for basin-scale water balance study: 2.
794 Evaluation on the Mississippi Basin and closure correction model. *Journal of Geophysical*
795 *Research: Atmospheres*, 119, 12,100-12,116, <http://dx.doi.org/10.1002/2014JD021953>.
- 796 Neal, J., Schumann, G., Bates, P., Buytaert, W., Matgen, P., Pappenberger, F., 2009. A data
797 assimilation approach to discharge estimation from space. *Hydrol. Process.*, 23, 36413649.
- 798 Oke, P.R., Sakov, P., Corney, S.P., 2007. Impacts of localisation in the EnKF and EnOI:
799 experiments with a small model. *Ocean Dyn.* 57, 3245.
- 800 Oke, P.R., Brassington, G.B., Griffin, D.A., Schiller, A., 2008. The Bluelink
801 Ocean Data Assimilation System (BODAS). *Ocean Modelling*, 21, 4670,
802 <http://dx.doi.org/10.1016/j.ocemod.2007.11.002>.
- 803 Ott, E., Hunt, B.R., Szunyogh, I., Zimin, A.V., Kostelich, E.J., Corazza, M., Kalnay, E., Patil,
804 D.J., Yorke, J.A., 2004. A local ensemble Kalman Filter for atmospheric data assimilation.
805 *Tellus*, 56A: 415-428.
- 806 Reager, J.T., Thomas, A.C., Sproles, E.A., Rodell, M., Beaudoin, H.K., Li, B., Famiglietti,
807 J.S., 2015. Assimilation of GRACE Terrestrial Water Storage Observations into a Land Sur-
808 face Model for the Assessment of Regional Flood Potential. *Remote Sens.*, 7, 14663-14679.
- 809 Renzullo, L.J., Van Dijk, A.I.J.M., Perraud, J.M., Collins, D., Henderson, B., Jin, H., Smith,
810 A.B., McJannet, D.L., 2014. Continental satellite soil moisture data assimilation improves
811 root-zone moisture analysis for water resources assessment. *J. Hydrol.*, 519, 27472762.
812 <http://dx.doi.org/10.1016/j.jhydrol.2014.08.008>.
- 813 Reichle, R. H., McLaughlin, D. B., Entekhabi, D., 2002. Hydrologic Data Assimilation with
814 the Ensemble Kalman Filter. *Mon. Wea. Rev.* 130, 103114, [http://dx.doi.org/10.1175/1520-](http://dx.doi.org/10.1175/1520-0493(2002)130;0103:HDAWTE;2.0.CO;2)
815 [0493\(2002\)130;0103:HDAWTE;2.0.CO;2](http://dx.doi.org/10.1175/1520-0493(2002)130;0103:HDAWTE;2.0.CO;2).

- 816 Reichle, R.H., Crow, W.T., Keppenne, C.L., 2008. An adaptive ensemble Kalman
817 filter for soil moisture data assimilation, *Water Resour. Res.*, 44, W03423,
818 <http://dx.doi.org/10.1029/2007WR006357>.
- 819 Reichle, R.H., Kumar, S.V., Mahanama, S.P.P., Koster, R.D., Liu, Q., 2010. Assimilation of
820 satellite-derived skin temperature observations into land surface models, *Journal of Hydrometeorology*, 11, 1103-1122, <http://dx.doi.org/10.1175/2010JHM1262.1>.
- 822 Reichle, R.H., De Lannoy, G.J., Forman, B.A., Draper, C.S., Liu, Q., 2013. Connecting satellite
823 observations with water cycle variables through land data assimilation: Examples using the
824 NASA GEOS-5 LDAS, in *The Earths Hydrological Cycle*, pp. 577606, Springer, Netherlands,
825 http://dx.doi.org/10.1007/978-94-017-8789-5_6.
- 826 Rodell, M., Houser, P.R., Jambor, U., Gottschalick, J., Mitchell, K., et al. (2004). The Global
827 Land Data Assimilation System, *Bull. Am. Meteorol. Soc.* 85, 381394.
- 828 Rodell, M., Chen, J., Kato, H., Famiglietti, J.S., Nigro, J., Wilson, C.R., 2007. Estimating
829 groundwater storage changes in the Mississippi River basin (USA) using GRACE. *Hydrogeol.*
830 *J.*, 15, 159166.
- 831 Rodgers, C.D., 2000. *Inverse Methods for Atmospheric Sounding: Theory and Practice*. World
832 Scientific, Singapore.
- 833 Sakov, P., Oke, P.R., 2008. A deterministic formulation of the ensemble Kalman filter: an
834 alternative to ensemble square root filters. *Tellus* 60A, 361371.
- 835 Schmidt, R., Petrovic, S., Gntner, A., Barthelmes, F., Wnsch, J., Kusche, J., 2008. Periodic
836 components of water storage changes from GRACE and global hydrology models. *J. Geophys.*
837 *Res.*, 113, B08419, <http://dx.doi.org/10.1029/2007JB005363>.
- 838 Schumacher, M., Kusche, J., Dll, P., 2016. A systematic impact assessment of
839 GRACE error correlation on data assimilation in hydrological models. *J Geodesy*.
840 <http://dx.doi.org/10.1007/s00190-016-0892-y>.
- 841 Schunk, R.W., Scherliess, L., Sojka, J.J., Thompson, D.C., 2004. USU global ionospheric data
842 assimilation models, *Atmospheric and Environmental Remote Sensing Data Processing and*
843 *Utilization: an End-to-End System Perspective*. (ed. H.-L. A. Huang and H. J. Bloom), *Proc.*
844 *of SPIE*, 5548, 327-336, <http://dx.doi.org/10.1117/12.562448>.

- 845 Seo, D.J., Koren, V., Cajina, N., 2003. Real-time variational assimilation of hydrologic and hy-
846 drometeorological data into operational hydrologic forecasting. *J. Hydrometeorol.*, 4, 627641.
- 847 Seoane, L., Ramillien, G., Frappart, F., Leblanc, M., 2013. Regional GRACE-based estimates
848 of water mass variations over Australia: validation and interpretation. *Hydrol. Earth Syst.*
849 *Sci.*, 17, 4925-4939, <http://dx.doi.org/10.5194/hess-17-4925-2013>.
- 850 Shannon, C.E., Weaver, W., 1949. *The Mathematical Theory of Communication*. University of
851 Illinois Press, Urbana.
- 852 Sheffield, J., Goteti, G., Wood, E.F., 2006. Development of a 50-year-high-resolution global
853 dataset of meteorological forcings for land surface modeling. *J. Clim.*, 19(13), 30883111.
- 854 Smith, A.B., Walker, J.P., Western, A.W., Young, R.I., Ellett, K.M., Pipunic, R.C., Richter,
855 H., 2012. The Murrumbidgee soil moisture monitoring network data set. *Water Resour. Res.*
856 48 (7), 16. <http://dx.doi.org/10.1029/2012WR011976>.
- 857 Stewart, L.M., Dance, S.L., Nichols, N.K., 2008. Correlated observation errors in data assimi-
858 lation. *Int. J. Numer. Meth. Fluids*, 56: 15211527. <http://dx.doi.org/10.1002/fld.1636>.
- 859 Stone, J.V., (2004). *Independent component analysis: a tutorial introduction*. MIT Press, Lon-
860 don.
- 861 Sun, Q., Xie, Z., Tian, X., 2015. GRACE terrestrial water storage data assimilation based on
862 the ensemble four-dimensional variational method PODEn4DVar: Method and validation.
863 *Sci. China Earth Sci.* 58: 371. <http://dx.doi.org/10.1007/s11430-014-4978-1>.
- 864 Swenson, S., Wahr, J., 2002. Methods for inferring regional surface-mass anomalies from Gravity
865 Recovery and Climate Experiment (GRACE) measurements of time-variable gravity. *Journal*
866 *of Geophysical research*, 107, B9, 2193. <http://dx.doi.org/10.1029/2001JB000576>.
- 867 Swenson, S., Wahr, J., 2006. Post-processing removal of correlated errors in GRACE data.
868 *Geophysical Research Letters*, 33, L08402. <http://dx.doi.org/10.1029/2005GL025285>.
- 869 Swenson, S., Chambers, D., Wahr, J., 2008. Estimating geocentervariations from a combina-
870 tion of GRACE and ocean model output. *Journal of Geophysical research*, 113, B08410.
871 <http://dx.doi.org/10.1029/2007JB005338>.

- 872 Syed, T.H., Famiglietti, J.S., Chen, J., Rodell, M., Seneviratne, S.I., Viterbo, P., Wil-
873 son, C.R., 2005. Total basin discharge for the Amazon and Mississippi River basins from
874 GRACE and a land-atmosphere water balance. *Geophysical Research Letters*, 32, L24404.
875 <http://dx.doi.org/10.1029/2005GL024851>
- 876 Tangdamrongsub, N., Steele-Dunne, S.C., Gunter, B.C., Ditmar, P.G., Weerts, A.H.,
877 2015. Data assimilation of GRACE terrestrial water storage estimates into a regional
878 hydrological model of the Rhine River basin. *Hydrol. Earth Syst. Sci.*, 19, 2079-2100,
879 <http://dx.doi.org/10.5194/hess-19-2079-2015>.
- 880 Tapley, B.D., Bettadpur, S., Watkins, M., Reigber, C., 2004. The gravity recovery and
881 climate experiment: mission overview and early results. *Geophys Res Lett* 31:L09607.
882 <http://dx.doi.org/10.1029/2004GL019920>.
- 883 Thomas, A.C., Reager, J.T., Famiglietti, J.S., Rodell, M., 2014. A GRACE-based water storage
884 deficit approach for hydrological drought characterization. *Geophys. Res. Lett.*, 41, 15371545.
- 885 Tippett, M.K., Anderson, J.L., Bishop, C.H., Hamill, T.M., Whitaker, J.S., 2003. Ensemble
886 square root filters. *Mon. Weath. Rev.*, 131, 148590.
- 887 Tregoning, P., McClusky, S., van Dijk, A.I.J.M., Crosbie, R.S., Pea-Arancibia, J.L., 2012.
888 Assessment of GRACE Satellites for Groundwater Estimation in Australia. National Water
889 Commission, Canberra, 82 pp.
- 890 van Dijk, A.I.J.M., 2010. The Australian Water Resources Assessment System: Technical Re-
891 port 3, Landscape model (version 0.5) Technical Description. CSIRO: Water for a Healthy
892 Country National Research Flagship.
- 893 van Dijk, A.I.J.M., Pea-Arancibia, J.L., Wood, E.F., Sheffield, J., Beck, H.E., 2013. Global
894 analysis of seasonal streamflow predictability using an ensemble prediction system and
895 observations from 6192 small catchments worldwide. *Water Resour. Res.*, 49, 27292746,
896 <http://dx.doi.org/10.1002/wrcr.20251>.
- 897 van Dijk, A.I.J.M., Renzullo, L.J., Wada Y, Tregoning, P., 2014. A global water cycle reanaly-
898 sis (2003–2012) merging satellite gravimetry and altimetry observations with a hydrological
899 multi-model ensemble. *Hydrol Earth Syst Sci* 18:29552973. [http://dx.doi.org/10.5194/hess-](http://dx.doi.org/10.5194/hess-18-2955-2014)
900 18-2955-2014.

- 901 van Leeuwen, P.J., Evensen, G., 1996. Data assimilation and inverse methods in terms of a
902 probabilistic formulation. *Monthly Weather Review* 124, 28982913.
- 903 Vrugt, J.A., Diks, C.G., Gupta, H.V., Bouten, W., Verstraten, J.M., 2005. Im-
904 proved treatment of uncertainty in hydrologic modeling: Combining the strengths
905 of global optimization and data assimilation. *Water Resour. Res.*, 41, W01017,
906 <http://dx.doi.org/10.1029/2004WR003059>.
- 907 Vrugt, J.A., ter Braak, C.J.F., Diks, C.G.H., Schoups, G., 2013. Advancing hydrologic data
908 assimilation using particle Markov chain Monte Carlo simulation: theory, concepts and
909 applications. *Advances in Water Resources, Anniversary Issue - 35 Years*, 51, 457-478,
910 <http://dx.doi.org/10.1016/j.advwatres.2012.04.002>.
- 911 Wahr, J., Molenaar, M., 1998. Time variability of the Earth's gravity field' Hydrological and
912 oceanic effects and their possible detection using GRACE. *Journal of Geophysical research*,
913 103, B12, 30, 205-30, 229. <http://dx.doi.org/10.1029/98JB02844>.
- 914 Watkins, M.M., Wiese, D.N., Yuan, D.-N., Boening, C., Landerer, F.W., 2015. Improved meth-
915 ods for observing Earths time variable mass distribution with GRACE using spherical cap
916 mascons. *J. Geophys. Res. Solid Earth*, 120, <http://dx.doi.org/10.1002/2014JB011547>.
- 917 Weerts, A.H., El Serafy, G.Y.H., 2006. Particle filtering and ensemble Kalman filtering for
918 state updating with hydrological conceptual rainfall-runoff models. *Water Resour. Res.*, 42,
919 W09403, <http://10.1029/2005WR004093>.
- 920 Widiastuti, E., 2009. Data assimilation of GRACE terrestrial water storage data into a hydro-
921 logical model using the ensemble Kalman smoother: A case study of the Rhine river basin.
922 MSc Thesis, TU Delft, Delft.
- 923 Wiese, D.N., 2015. GRACE monthly global water mass grids NETCDF RE-
924 LEASE 5.0. Ver. 5.0. PO.DAAC, CA, USA. Dataset accessed [YYYY-MM-DD] at
925 <http://dx.doi.org/10.5067/TEMSC-OCL05>.
- 926 Wouters, B., Bonin, J.A., Chambers, D.P., Riva, R.E. M., Sasgen, I., Wahr, J., 2014. GRACE,
927 time-varying gravity, Earth system dynamics and climate change. *Reports on Progress in*
928 *Physics*, 77, 11, 116801. <http://dx.doi.org/10.1088/0034-4885/77/11/116801>.

- 929 Zaitchik, B.F., Rodell, M., Reichle, R.H., 2008. Assimilation of GRACE terrestrial water storage
930 data into a land surface model: results for the Mississippi River Basin. *J. Hydrometeorol*
931 *9*(3):535-548. <http://dx.doi.org/10.1175/2007JHM951.1>.
- 932 Zeng, Y., 2014. Efficient Radar Forward Operator for Operational Data Assimilation within
933 the COSMO-model, KIT Scientific Publishing. pp. 187. ISBN 3731501287, 9783731501282.
- 934 Zhang, Y., Bocquet, M., Mallet, V., Seigneur, C., Baklanov, A., 2012. Real-time air quality
935 forecasting, Part I: History, techniques, and current status. *Atmos. Environ.*, *60*, 632655.

ACCEPTED MANUSCRIPT

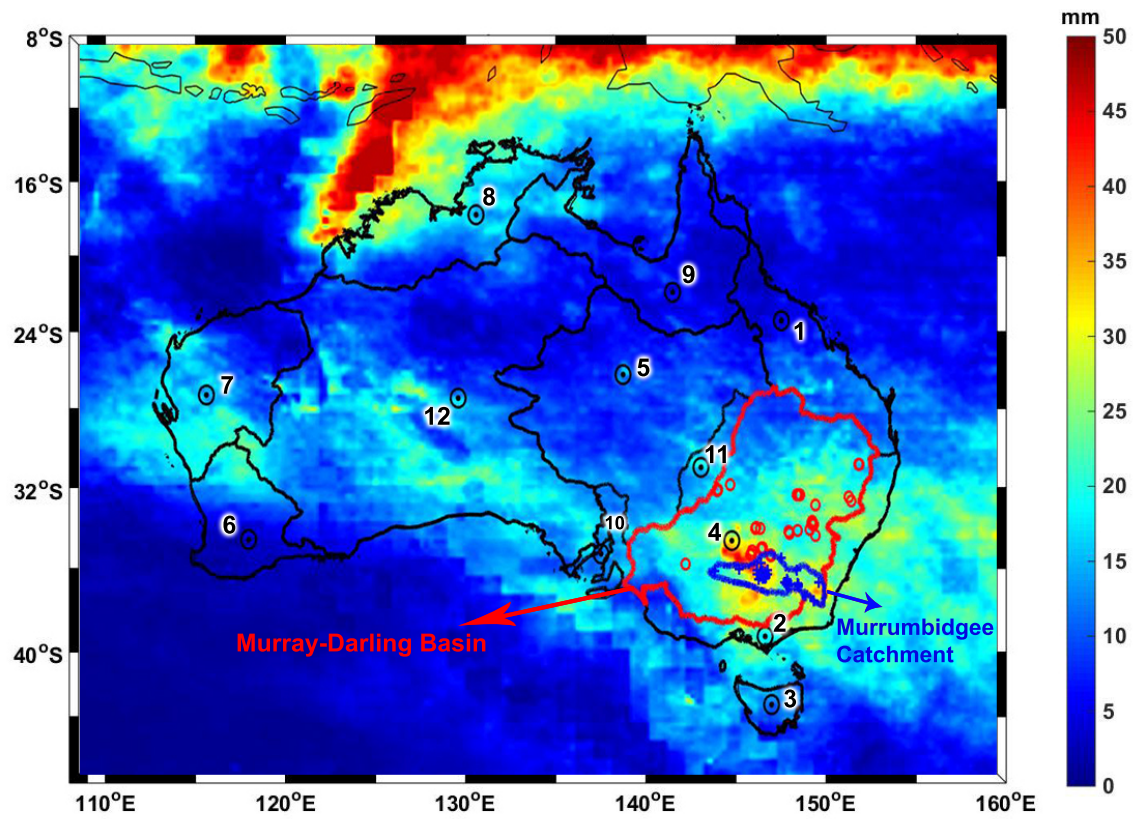


Figure 1: Overview of the study area. The black polygons indicate the twelve river basins that are considered for spatial aggregation of GRACE data to basin scale. The red and blue polygons indicate the Murray-Darling Basin and Murrumbidgee Catchment, respectively. Data from in-situ groundwater stations (red circles) and data from the OzNet soil moisture network (blue circles) are used in these regions for independent validation of the data assimilation results. The underlying map shows temporally averaged precipitation between 2003-2013 from TRMM-3B42 products (Huffman et al., 2012) on a $1^\circ \times 1^\circ$ grid.

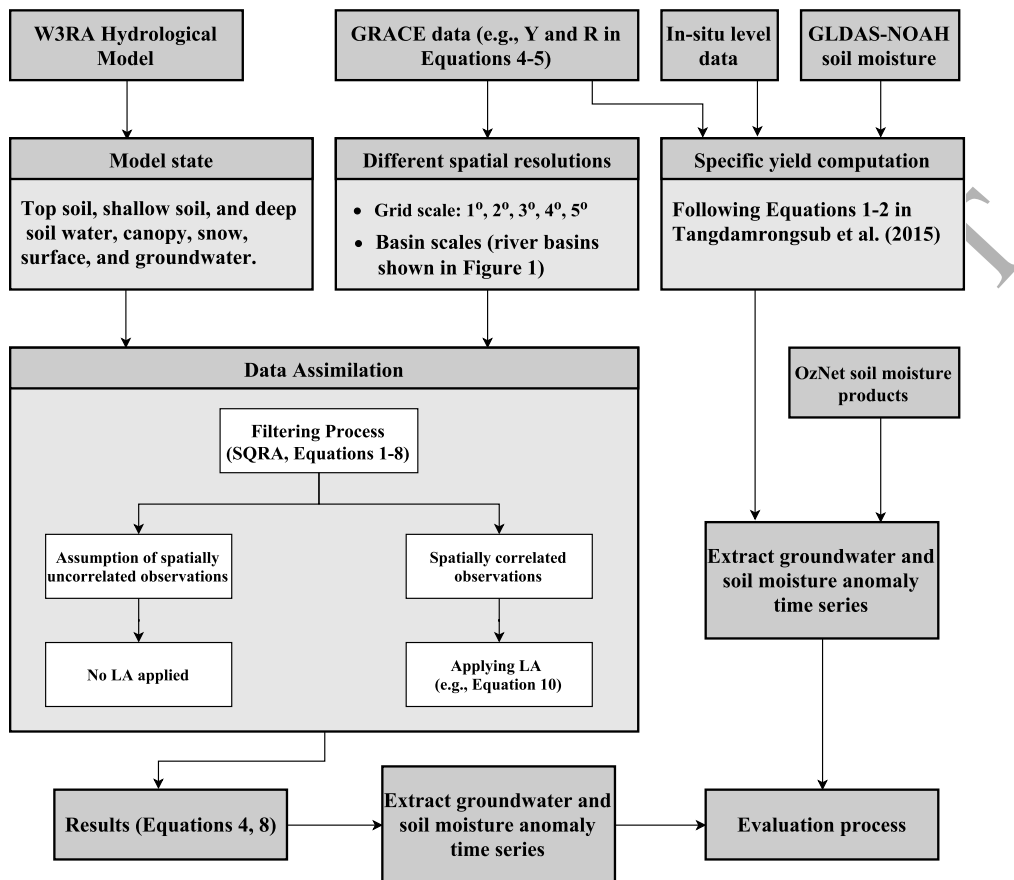


Figure 2: A schematic illustration of the data assimilation approach implemented for this study and of the considered data sets.

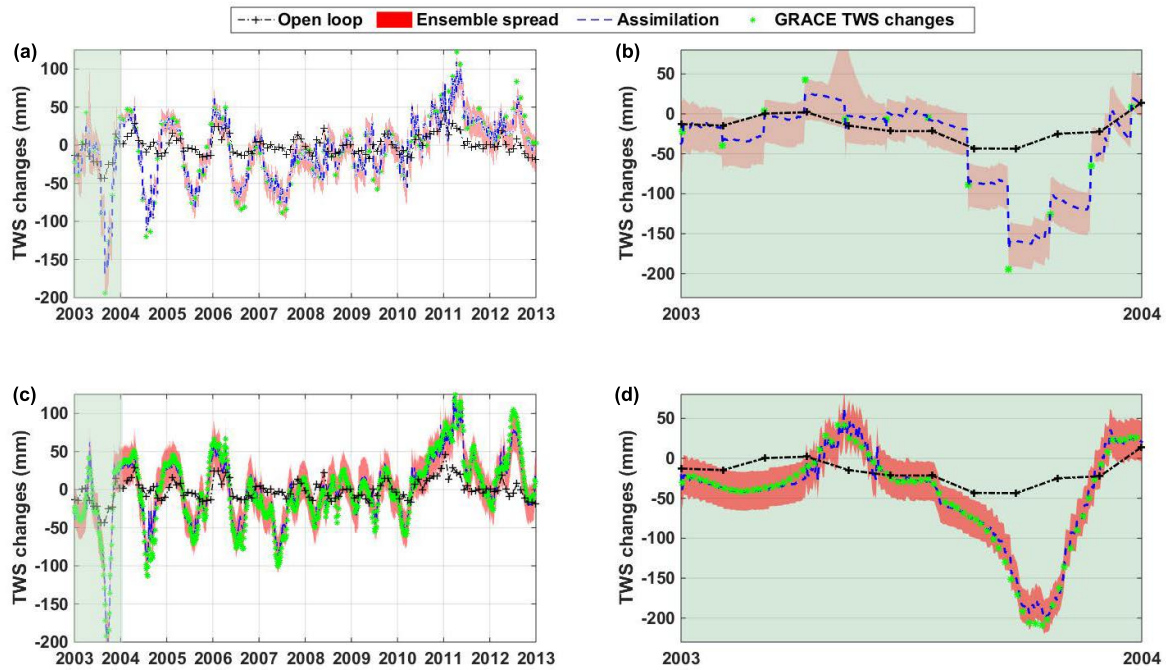


Figure 3: Comparison between the assimilated time series using the 1° observations in a monthly (a) and 5-day temporal scale for an arbitrary point (c). (b) and (d) respectively magnified the green areas of (a) and (c) representing a zoom-in for one year. Ensemble spread represents the spread of the ensemble of updated TWS states. Note that we use LA to account for correlated errors in GRACE error covariance for this figure.

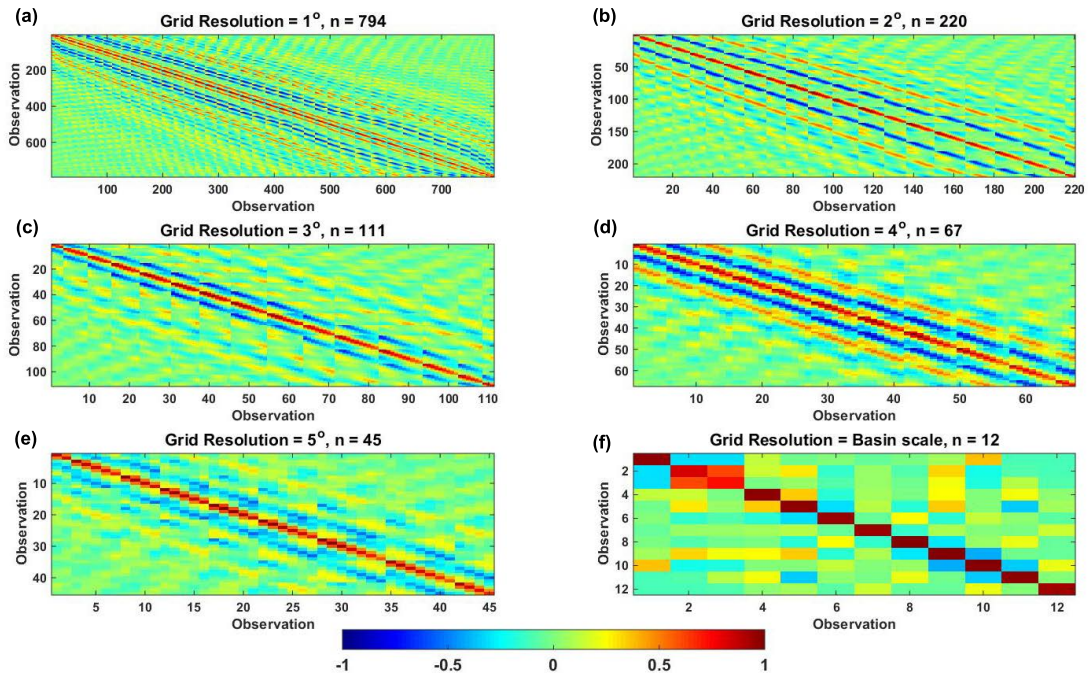


Figure 4: Correlation matrices of the GRACE observations corresponding to various spatial aggregations. Here, no localization is applied. The variable n refers to the number of assimilated observations.

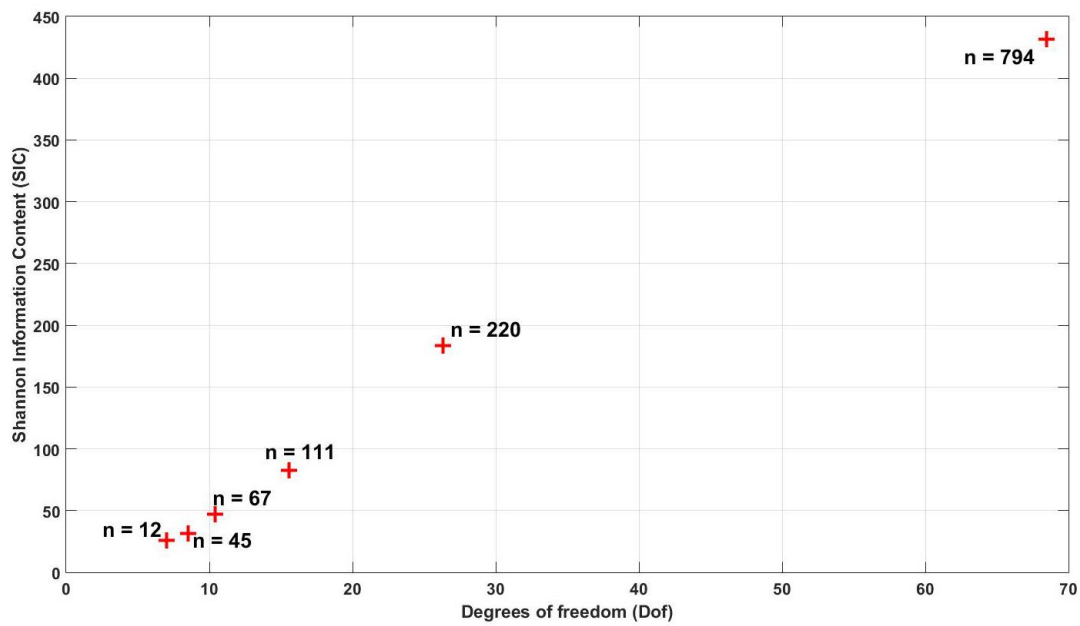


Figure 5: Shannon Information Content (SIC) and Degrees of freedom (Dof) with respect to the number of assimilated GRACE observations (n).

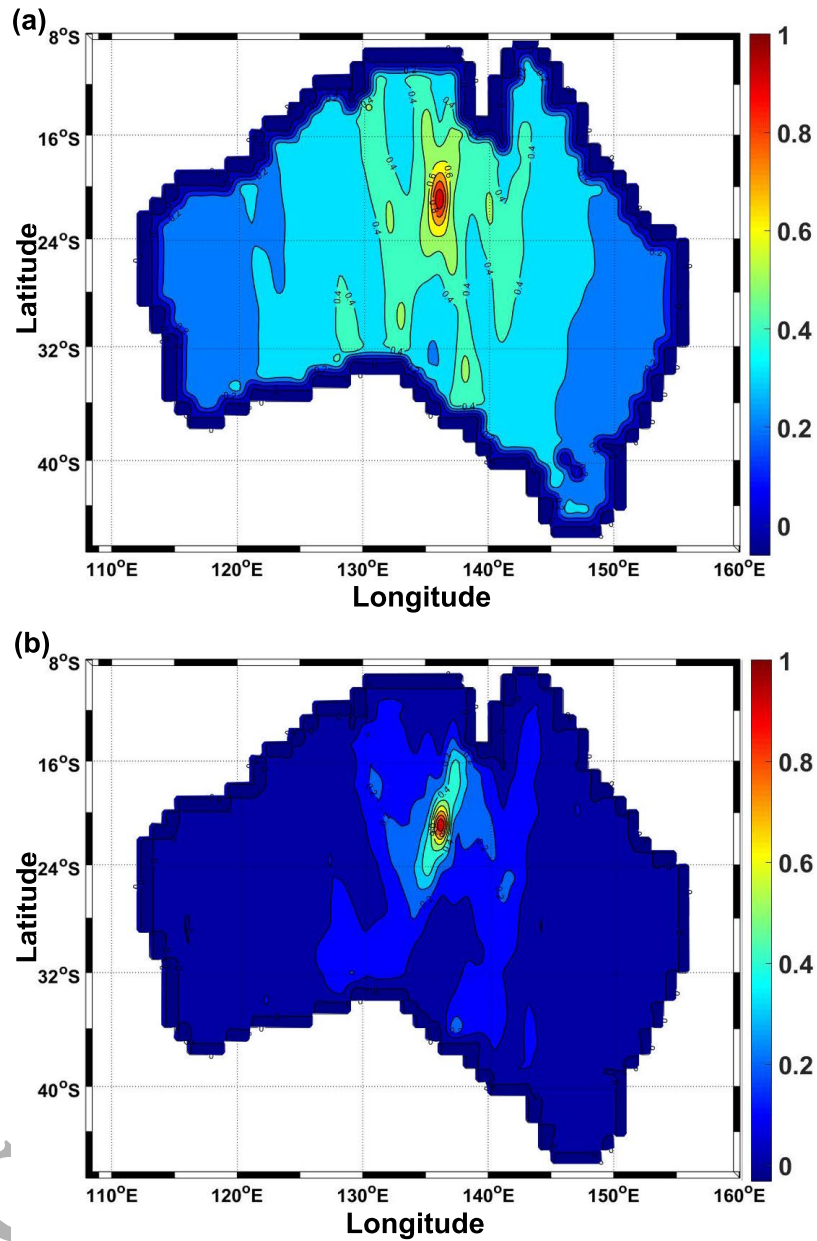


Figure 6: 2-D representation of correlation coefficients between the TWS anomalies of the arbitrary point (136.6854°E and 23.9015°S) and the rest of the grid points. The temporal average of the correlation coefficients before and after assimilation using LA are shown in (a) and (b) respectively.

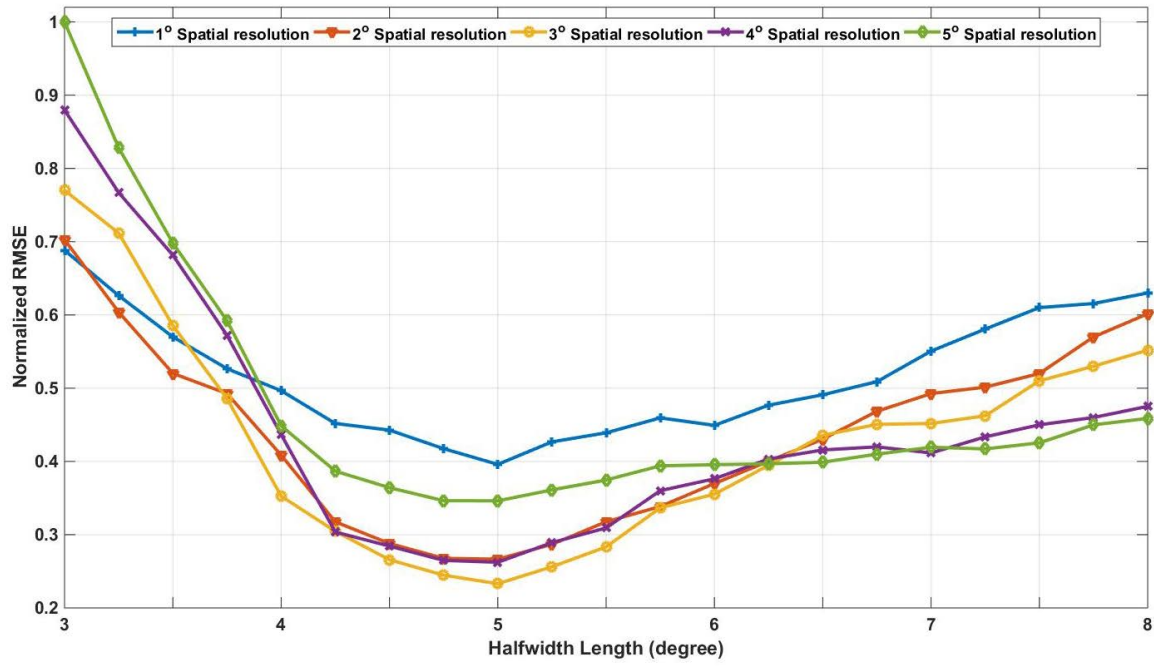


Figure 7: Comparison between normalized RMSE of TWS anomalies for different localisation radii (degree) applied for each case of GRACE TWS spatial resolution used for assimilation. RMSEs are calculated in mm, however, for a better visual presentation, normalized values are presented.

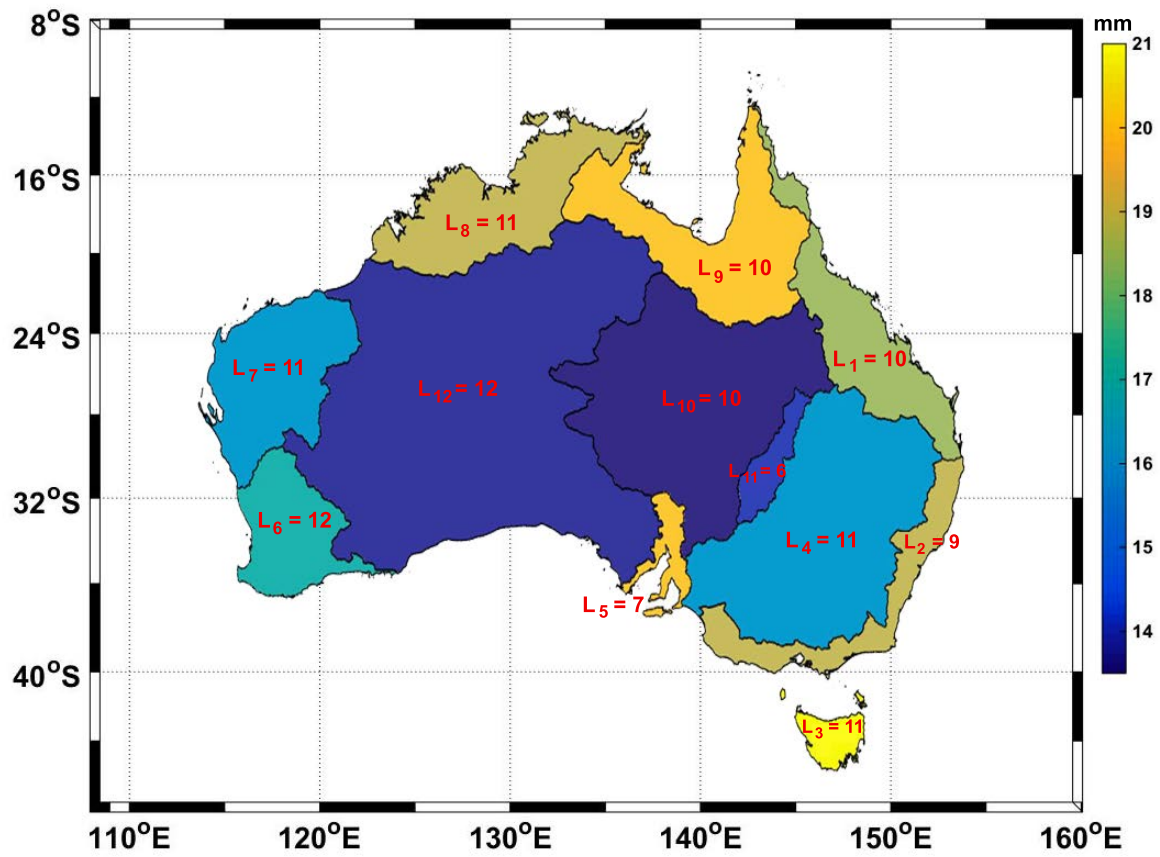


Figure 8: The estimated optimized localisation radii (in degree and presented by L) and corresponding TWS errors with respect to the GRACE data for each basin.

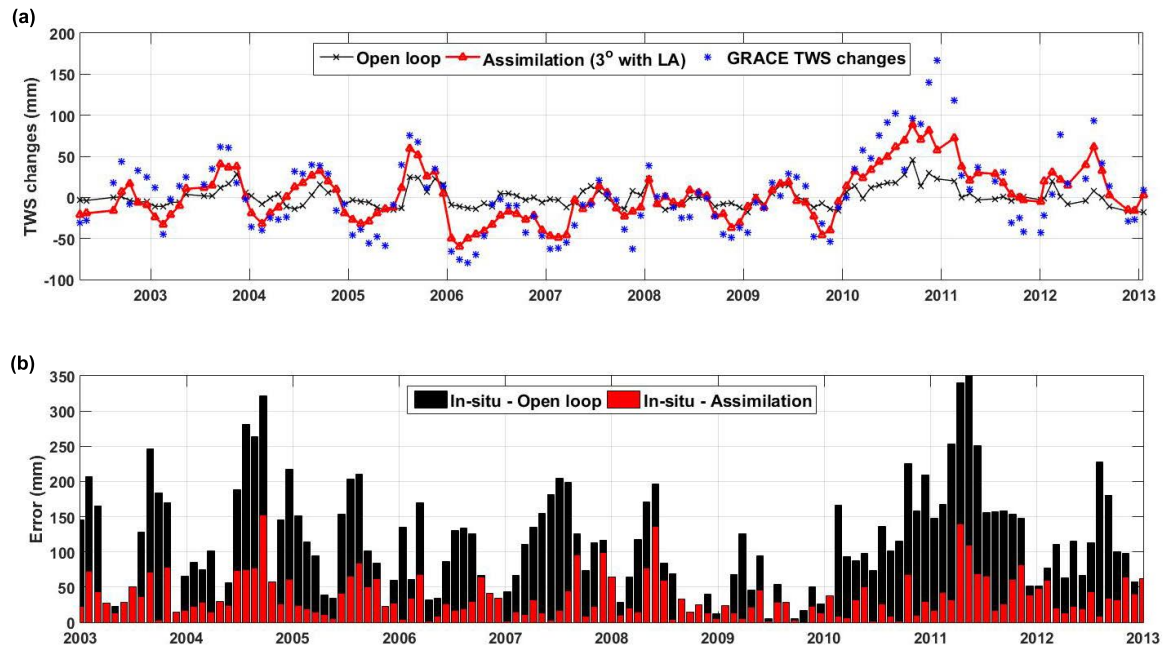


Figure 9: (a) Comparison between the TWS time series of the assimilation process for the case of 3° spatial resolution (red), the GRACE observation (blue), with the open loop referring to the model estimation without applying data assimilation (black). (b) Absolute groundwater (GW) error bars before (black) and after (red) data assimilation process in comparison to the GW in-situ measurements. The time series shown in (a) and (b) are spatially averaged over the Murray-Darling Basin.

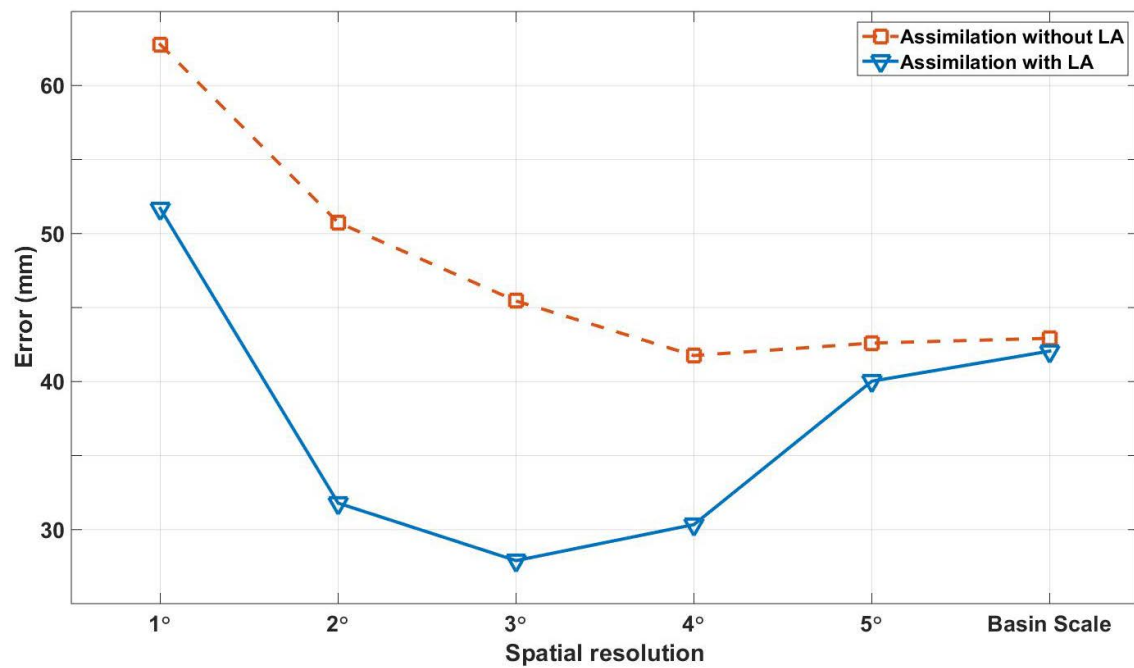


Figure 10: Average estimated error in groundwater anomalies from assimilating GRACE data for different spatial scales with (blue) and without (red) implementation of LA. The results are spatial averages over all groundwater data points within the Murray-Darling Basin.

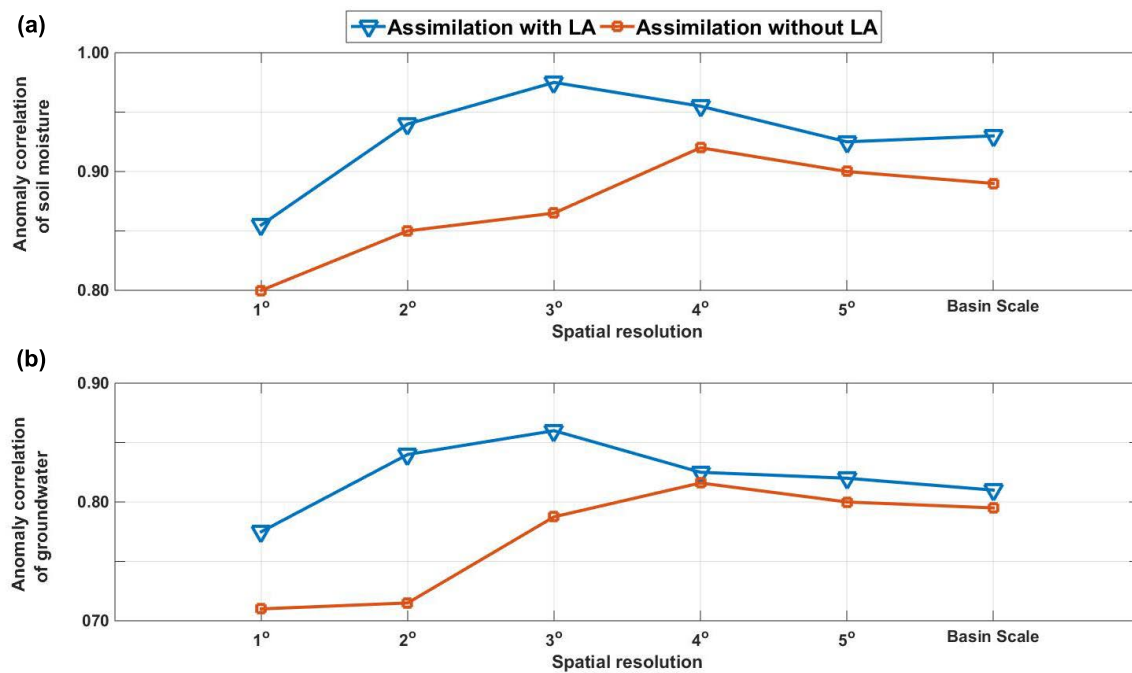


Figure 11: Comparison between the correlation of assimilation results (using different spatial resolutions) with OzNet soil moisture anomalies spatially averaged over the Murrumbidgee Catchment (a) and with anomalies of groundwater in-situ level measurements spatially averaged over the Murray-Darling Basin (b). The correlation results in both cases of data assimilation using LA (blue) and without using LA (red) are shown.

Table 1: The details of GRACE observations used in each grid resolution.

Spatial Scale	Observation Number	Rank	LA Rank*
1°	794	268	794
2°	220	211	220
3°	111	111	111
4°	67	67	67
5°	45	45	45
<i>BasinScale</i>	12	12	12

* Computed rank after the implementation of LA.

Table 2: A summary of the results belonging to each scenario of data assimilation. Improvements in groundwater are calculated using the estimated RMSE with and without applying data assimilation (open loop) in relation to groundwater in-situ measurements.

Spatial Scale	Assimilation without LA		Assimilation with LA	
	RMSE (mm)	Improvement (%)	RMSE (mm)	Improvement (%)
1°	68.54	17.76	52.23	37.33
2°	51.09	38.70	35.11	57.87
3°	47.41	43.11	26.80	67.84
4°	43.18	48.19	32.35	61.18
5°	44.37	46.76	41.19	50.58
<i>BasinScale</i>	43.84	47.40	41.93	49.69